Title
PTEN and the Emergence of Cortical Perisomatic Inhibition

Author
Baohan, Amy

Publication Date
2014

Peer reviewed|Thesis/dissertation

UNIVERSITY OF CALIFORNIA

Los Angeles

PTEN and the Emergence of Cortical Perisomatic Inhibition

A dissertation submitted in partial satisfaction of the

requirements for the degree Doctor of Philosophy in

Neuroscience

by

Amy Baohan

2014

Abstract

PTEN and the Emergence of Perisomatic Inhibition

by

Amy Baohan

Doctor of Philosophy in Neuroscience

University of California, Los Angeles, 2014

Professor Joshua T. Trachtenberg, Chair

Adequate perisomatic inhibition in the cortex, as supplied by parvalbumin-expressing (PV) inhibitory neurons, is fundamental to critical period plasticity and cortical function. Yet, how perisomatic inhibition emerges just at the inception of the critical period to shape the structure and function of cortical circuits is little understood. We report that PTEN in PV cells serves as a regulator of perisomatic inhibition by controlling the expression of EphB4, an inhibitor of PV to pyramidal inhibitory synapse formation. This points to a molecular disinhibitory mechanism for the initiation of the critical period, whereby sensory experience acts on PTEN in PV cells to decrease EphB4 expression in order to reduce the native repulsion between PV presynaptic terminals and pyramidal neuron cell bodies. This would then permit the formation of adequate

perisomatic inhibition in cortical circuits. Given the compelling link between deficits in cortical perisomatic inhibition and various psychiatric disorders, such as autism spectrum disorders and schizophrenia, our findings also recommend EphB4 in PV cells as a novel target of therapy.

This dissertation of Amy Baohan is approved.

Carlos Portera-Cailliau

Andrew Charles

Michael Levine

Joshua T. Trachtenberg, Committee Chair

It was the best of times, it was the worst of times,

It was the age of wisdom, it was the age of foolishness,

It was the epoch of belief, it was the epoch of incredulity,

It was the season of Light, it was the season of Darkness,

It was the spring of hope, it was the winter of despair,

We had everything before us, we had nothing before us,

We were all going direct to Heaven,

We were all going direct the other way…

A Tale of Two Cities

Charles Dickens

Table of Contents

List of Figures

Acknowledgements

This project, dissertation, and PhD would not have been possible without the support, guidance, and advice (solicited and otherwise) of Josh Trachtenberg. Many thanks also go to Taruna Ikrar, Xiangmin Xu, Vivek Swarup, Revital Versano, Peyman Golshani, Elaine Tring, and other members of the Trachtenberg lab.

Last but not least, my deepest gratitude goes to my parents for their unconditional support for the past quarter of a century.

VITA

2009 BA, Neuroscience,
summa cum laude
Columbia University

Publications

Chen, T.W., Wardill, T.J., Sun, Y., Pulver, S.R., Renninger, S.L., **Baohan, A.,** Schreiter, E.R., Kerr, R.A., Orger, M.B., Jayaraman, V., Looger, L.L., Svoboda, K., Kim, D.S. Ultra-sensitive fluorescent proteins for imaging activity in neuronal populations and synapses. *Nature* **499(7458)**, 295- 300 (2013).

Kholodilov, N., Kim, S.R., Yarygina, O., Kareva, T., Cho, J.W., **Baohan, A.**, Burke, R.E. Glial cell line-derived neurotrophic factor receptor-α1 expressed in striatum in trans regulates development and injury response of dopamine neurons of the substantia nigra. *J Neurochem* **116(4),** 486-98 (2011).

Ries, V., Cheng, H.C., **Baohan, A.**, Kareva, T., Oo, T., Rzhetskaya, M., Bland, R., During, M., Kholodilov, N., Burke, R.E. Akt/Protein Kinase B regulates the postnatal development of dopamine neurons of the substantia nigra in vivo. *J Neurochem* **110(1),** 23-33 (2009).

Chapter I

Introduction

Cortical inhibition

Excitatory (pyramidal) and inhibitory neurons constitute the two major neuronal populations in the cortex. While pyramidal neurons are the key mediators of information transfer within and between cortical regions, their activity is stringently modulated by inhibitory neurons, which via the release of GABA control the spatiotemporal range of excitation (Pouille and Scanziani, 2009; Isaacson and Scanziani, 2011). Excitation and inhibition are in fact inseparable (Abbott and Chance, 2005). Feed-forward and recurrent inhibition ensure that any excitation in a circuit is accompanied by concurrent inhibition. This coordination of excitation and inhibition is crucial for normal cortical function (Gabernet et al., 2005, Okun and Lampl, 2008; Yizhar et al., 2011).

Cortical inhibition is generated by a diverse group of cells with distinct molecular, electrophysiological, and anatomical properties that form distinct microcircuits (Markram et al., 2001). Classification of inhibitory neurons is nebulous and has been done by expression of unique molecular markers (parvalbumin, somatostatin, vasoactive intestinal peptide, cholecystokinin), neuromodulatory receptors (i.e. 5HT3aR), anatomic properties and firing patterns, to name a few criteria (Ascoli et al., 2008; Burkhalter 2008; Lee et al., 2010; Petersen and Crochet, 2013; Markram et al., 2001; DeFelipe et al., 2013). Henceforth, inhibitory neurons will be referred to by their expression of molecular markers.

Medial ganglionic eminence-derived somatostatin expressing neurons (SOM) and parvalbumin expressing neurons (PV) together account for almost all of cortical inhibition. SOM neurons (some of which are also called Martinotti cells) have regular,

adapting firing patterns and form a microcircuit with pyramidal, PV, and VIP neurons, such that they inhibit pyramidal and PV cells and are in turn inhibited by VIP neurons and excited by pyramidal neurons (**Fig. 1a**; Acsady et al., 1996; Freund and Buzsáki, 1996; Staiger et al., 2004; Pfeffer and Scanziani, 2013; Pi et al., 2013, Fino and Yuste, 2011). Somatostatin inhibitory neurons supply inhibition to the distal apical dendrites of nearby pyramidal neurons, thereby regulating the cortico-cortical input onto these neurons (**Fig. 1b**; Larkum et al., 1999; Larkum et al., 2009; Losonczy et al., 2008; Branco and Hausser, 2011). This also endows SOM neurons with the ability to regulate the extent of burst spiking of pyramidal neurons (Silberberg and Markram, 2007; Wang et al., 2004; Gentet et al., 2010).

PV cells account for the vast majority of inhibition by most accounts (Markram et al., 2001; Gonchar and Burkhalter, 1997). Activation of PV cells alone across the cortex via channelrhodopsin-2 is apparently sufficient to induce cortical quiescence (Lien and Scanziani, 2012). PV cells have a fast, non-adaptive firing pattern, with narrow action potentials and deep, sharp afterhyperpolarizations (Pangratz-Fuehrer and Hestrin, 2011). They receive input from pyramidal neurons, other PV cells, SOM cells, and to a marginal extent, VIP cells (**Fig. 1a**; David et al., 2007; Hofer et al., 2011; Pangratz-Fuehrer and Hestrin, 2011; Kawaguchi and Kubota, 1997; Pfeffer and Scanziani, 2013; Pi et al., 2013). In turn, PV cells inhibit pyramidal neurons and to a lesser extent, other PV cells (**Fig. 1a**; Packer and Yuste, 2011; Hofer et al., 2011; Pfeffer and Scanziani, 2013). They can be further subdivided into basket and chandelier cells, which innervate the cell body and axon initial segment, respectively (**Fig. 1b**; Somogyi 1977; Cirsto et al., 2004;

Taniguchi et al., 2013). Both control the output of postsynaptic neurons (Kvitsiani et al., 2013). Another unique property of PV circuits is the presence of gap junctions linking PV cells with each other, the computational function of which is unclear (Figure 1A; Hestrin and Galarreta, 2005; Sippy and Yuste, 2013).

Different forms of inhibition: somatostatin

Given that different inhibitory neurons receive different feed-forward input, form distinct microcircuits, and innervate different sub-compartments of pyramidal neurons, it is not surprising that they have different functions in a local cortical circuit (Xu and Callaway 2009). In the primary visual cortex (V1), moderately orientation-tuned SOM cells mediate surround suppression, the process whereby concurrently stimulating the area outside the receptive field of a neuron decreases the response of that neuron to a stimulus in the center of the receptive field (Ma et al., 2010; Adesnik et al., 2012). The receptive field size of neurons is the size of visual stimuli to which neurons preferentially respond and in V1, this property is determined primarily by feed-forward thalamic input, which means that the phenomenon of surround suppression has a subcortical origin (Hubel and Wiesel, 1959). However, local cortical circuitry, namely dense, lateral SOM inhibition of pyramidal neurons further builds upon that process in the cortex (Adesnik et al., 2012). The receptive field size of SOM neurons is almost four times greater than that of pyramidal neurons (80° vs. 21°). Together with the fact that near concurrent activation of pyramidal and inhibitory neurons occurs with visual input, this property of SOM neurons allows them to suppress the activity of pyramidal neurons in response to visual

stimuli approximating the size of the SOM receptive field, thereby maintaining the small receptive field size of pyramidal neurons (Adesnik et al., 2012). In other words, increasingly larger stimuli increasingly recruit SOM cells, most likely via increasing feed-forward input, thereby inhibiting local pyramidal neurons, resulting in the maintenance of the small receptive field size of pyramidal neurons (Adesnik et al., 2012). Indeed, optogenetically decreasing SOM population activity with archaerhodopsin (a light activated proton pump) in V1 increases the receptive field of pyramidal neurons without changing the preferred receptive field size, suggesting that while lateral inhibition via local cortical circuitry regulates surround suppression, there is still a distinct subcortical component (Adesnik et al., 2012). Meanwhile, manipulating the activity of PV cells, which have a similar receptive field size to that of pyramidal neurons, has no effect on surround inhibition (Adesnik et al., 2012).

The contribution of SOM neurons to the orientation tuning of pyramidal neurons in V1 is controversial. While some have shown that optogenetically increasing the activity of L2/3 SOM cells with channelrhodopsin (a light activated cation channel) decreases the tuning width and increases the orientation and direction selectivity of surrounding L2/3 pyramidal neurons, others have failed to show the same effect with a similar method of manipulation, namely optogenetics (Wilson et al., 2012; Lee et al., 2012). The discrepancy in findings can perhaps be attributed to a difference in recording modality (Ca^{2+} imaging vs. multiunit recordings) and also to the extent and duration of optogenetic manipulation of SOM activity (Wilson et al., 2012; Lee et al., 2012; Lee et al., 2014).

In the barrel cortex, SOM neurons hyperpolarize in response to whisking, both passive and active (Gentet et al., 2012). In the absence of whisking, they are the only active cells in the circuit, pointing to a role for SOM cells in generating tonic inhibition in periods of behavioral quiescence (Gentet et al., 2010; Gentet et al., 2012). Inhibition of SOM cells with halorhodopsin (a light activated chloride channel) engenders burst spiking in nearby pyramidal neurons. This suggests that the absence of SOM activity during whisking may promote sensorimotor integration via non-linear dendritic processing of inputs from the motor cortex located on distal apical dendrites of L5 pyramidal neurons, resulting in local dendritic spiking, which then generates burst-spiking (Larkum et al., 1999; Wang et al., 2004; Petersen 2008; Larkum et al., 2009; Losonczy et al., 2008; Branco and Hausser, 2011; Gentet et al., 2012; Xu et al., 2012).

PV inhibition

In primary sensory cortices, PV cells linearly modulate the activity of pyramidal neurons, thereby regulating gain, one of the many computations performed by the cortex (**Fig. 1c**; Ayaz and Chance 2008; Kerlin et al., 2010; Atallah et al., 2012; Wilson et al., 2012; Carandini and Heeger, 2013). In the primary visual cortex, PV cells receive distributed input from diversely tuned pyramidal neurons, which endows them with their broad orientation tuning (Niell and Stryker, 2008; Kerlin et al., 2010; Chen et al., 2013). In turn, they supply diffuse perisomatic inhibition to pyramidal neurons in response to visual stimuli of all orientations (Kerlin et al., 2010 Hofer et al., 2011; Packer and Yuste, 2011; Chen et al., 2013). Bidirectionally modulating PV population activity with

channelrhodopsin-2 and archaerhodopsin in the primary visual cortex linearly modulates the activity of pyramidal neurons without altering their contrast sensitivity, tuning preference and width, or direction selectivity (Atallah et al., 2012). This function of PV cells is also seen in other regions of the brain, such as the olfactory bulb, where input-output transformations can be studied. Like PV cells in the visual cortex, olfactory bulb PV cells are also broadly tuned and highly connected to surrounding excitatory neurons, the mitral cells (Packer and Yuste, 2011; Kato et al., 2013). Pharmacogenetic reduction of PV activity with PSEM in the olfactory bulb linearly increases excitatory neuron responses to odor without affecting odor preference (Kato et al., 2013). Taken together, this points to a role for PV cells in mediating context invariant sensory processing in primary sensory areas, such as contrast invariant orientation and direction selectivity of pyramidal neurons in the primary visual cortex, which is crucial for an animal's ability to recognize the same visual stimuli under different lighting conditions.

PV-pyramidal reciprocal interaction also gives rise to gamma oscillations in the cortex. Gamma oscillations are rhythmic fluctuations of local field potential (LFP) in the 30-90 Hz range and reflect summed sub- and supra-threshold activity of a network. As such, it is likely an epiphenomenon of circuit activity during certain brain states such as attentive wakefulness and sensory processing, although some models suggest that LFP oscillation itself increases a circuit's signal-to-noise ratio and facilitates transfer of information across the cortex via long-range phase coherence (Engel et al., 2001; Sirota et al., 2008; Sohal et al., 2009; Atallah and Scanziani, 2009; Buzsaki and Wang, 2012). While many models can explain the origin of gamma oscillations, the requisite elements

of most include PV basket cells, PV-pyramidal reciprocal connectivity, and PV-PV reciprocal connectivity of either the gap junction or synaptic variety (Buzsaki et al. 1983, Bragin et al. 1995, Hasenstaub et al. 2005, Freund & Katona 2007, Atallah and Scanziani, 2009; Cardin et al., 2007; Buzsaki and Wang, 2012). A combination of the I-I and E-I models suggests that gamma oscillations arise from common, synchronous excitatory input onto PV cells, which via their divergent connections to pyramidal neurons, generate synchronous IPSPs (Buzsaki and Wang, 2012). The resulting gamma LFP is a pastiche of coordinated APs (PV cells) and IPSPs (pyramidal). Gap junctions amongst PV cells may serve to augment PV synchrony, while the function of mutual synaptic inhibition amongst PV cells is contentious but may also be to synchronize PV cells (Buzsaki and Wang, 2012). Gamma LFP is a convenient read-out of network dynamics since it is evidently non-PV autonomous. Ramp activation of L2/3 pyramidal neurons *in vivo* via channelrhodopsin-2 can generate gamma rhythms, presumably through the gradual recruitment of PV inhibition (Adesnik and Scanziani, 2010). In contrast to phasic activation at frequencies that exceed their physiological spiking capacity, ramp activation of pyramidal neurons allows them to function within their physiological spiking range, which may explain why stimulating pyramidal neurons at the gamma frequency of 40 Hz fails to elicit gamma LFPs while stimulating fast-spiking PV cells, which have a much higher spiking capacity than pyramidal neurons, at the same frequency can (Sohal et al., 2009; Cardin et al., 2009). Attenuated gamma oscillations are seen in mouse models of psychiatric diseases such as schizophrenia and likely reflect anomalous circuit dynamics.

PV cells also participate in a number of disinhibitory circuits important in sensory

plasticity, gating, and learning (**Fig. 2**). Disinhibition via PV cells can occur in two ways: decreased excitation of PV cells and/or increased inhibition of PV cells (**Fig. 2**). Ocular dominance plasticity in V1, for example, is facilitated by decreased feed-forward excitation of PV cells, which results in the disinhibition of surrounding pyramidal neurons (**Fig. 2b**; Kuhlman et al., 2013). Pharmacogenetic reduction of PV activity in adult mice with monocular deprivation can induce ocular dominance plasticity, which ordinarily occurs only during the critical period (P23-30) (Kuhlman et al., 2013).

An example of increased inhibition of PV cells is the increased L1 inhibitory neuron input to PV cells in L2/3 during fear conditioning, which appears to be necessary to increase the saliency of sensory stimuli (**Fig. 2a**; Letzkus et al., 2011). Foot shocks increase basal forebrain cholinergic input to L1 inhibitory neurons, which then inhibit PV cells and disinhibit pyramidal neurons. The decreased activity of PV cells and increased activity of pyramidal neurons during learning may underlie sparser but stronger coding of sensory stimuli following learning (Gdalyahu et al., 2012). PV cells are also downstream of SOM and to a lesser extent, VIP neurons, both of which are also loci of disinhibitory control (**Fig. 2a**). SOM neurons in L4, the thalamorecipient layer, preferentially inhibit PV cells, unlike supragranular and infragranular SOM cells which preferentially inhibit the apical dendrites of pyramidal neurons (Xu et al., 2012). This combined with the observation that SOM cells are strongly modulated by cholinergic inputs from the basal forebrain point to a role for SOM cells in in gating sensory input from the thalamus by disinhibiting excitatory neurons via inhibition of PV cells in states of attention and arousal (**Fig. 2a**; Fanselow et al., 2008; Xu et al., 2012).

The extent and function of VIP inhibition of PV cells is a source of contention (David et al., 2007; Pi et al., 2013; Pfeffer and Scanziani, 2013). Work in the primary visual cortex *in vitro* suggests that the VIP input to PV cells is minimal. However, in the auditory cortex *in vivo*, VIP neurons can disinhibit pyramidal neurons via both SOM and PV cells during learning (**Fig. 2a**). Specifically, VIP cells respond only during the presentation of reinforcement signals in an auditory go-no go discrimination task, thereby transiently disinhibiting pyramidal neurons (Pi et al., 2013). Since VIP cells receive cholinergic input from the basal forebrain, the finding suggests that VIP activity may be attention dependent, which may also account for why it seemingly has a greater control over downstream inhibitory neurons *in vivo* than *in vitro* (Pi et al., 2013; Pfeffer and Scanziani, 2013).

Lastly, *in vivo* recordings of PV cells in association cortices of freely roaming rodents have revealed behavioral and decision-making correlates of PV population activity. Multiunit recordings in the anterior cingulate cortex, an area implicated in foraging related decision-making, during a task that mimics natural foraging reveal that PV cells preferentially spike as the mouse is leaving the reward zone and that the response is graded, with the activity of PV cells increasing linearly with longer staying times in the reward zone (Kvitsiani et al., 2013). Meanwhile, SOM activity has a different behavioral correlate. A subpopulation of SOM cells with relatively narrow action potentials responds selectively as mice approach the reward zone (Kvitsiani et al., 2013). Although these findings are correlational, they are some of the first evidence for PV and SOM specific functions in an association cortex and suggest that PV and SOM cells

regulate information flow and participate in some aspect of cortical computation associated with decision-making (Constantinidis et al., 2002; Kvitsiani et al., 2013).

PV cells, inhibition & psychiatric disorders

The importance of inhibition can further be highlighted by the fact that an imbalance in excitation and inhibition (E/I) is associated with a variety of neurologic and psychiatric disorders. When excitation greatly supersedes inhibition, seizures can arise, whereas more subtle forms of E/I imbalance are associated with the social and cognitive deficits seen in schizophrenia and autism spectrum disorders (ASD) (Yizhar et al., 2011; Lewis et al., 2012). In fact, many autistic patients display atypical hyperactivity in frontal association cortices and up to 30% experience seizures (Yizhar et al., 2011; Belmonte et al., 2010; Gomot et al., 2008; Canitano, 2007).

Of the inhibitory neurons, PV cells are the most strongly associated with psychiatric disease. The social, cognitive, and behavioral deficits associated with autism spectrum disorders and schizophrenia can be modeled in mice by increasing the excitability of pyramidal neurons in the medial prefrontal cortex (mPFC) with a bistable step function opsin, thereby disrupting the native excitation to inhibition balance in the circuit. Notably, these deficits can be rescued by concurrently increasing the activity of PV cells and restoring the excitation to inhibition balance (Yizhar et al., 2011). Deficits in PV inhibition are also seen in a mouse model of Fragile X syndrome, which causes a

syndromic form of autism. Specifically, a 20% reduction in the number of neocortical PV cells is observed as a consequence of non-specifically knocking out *FMR1,* which codes for a protein that acts as a negative regulator of translation.

In addition to disrupting the excitation to inhibition balance in cortical circuits, schizophrenia can also be modeled by selectively mutating *ErbB4*, a schizophrenia susceptibility gene that encodes a receptor tyrosine kinase, in just PV inhibitory neurons (del Pino et al., 2013). Double copy *ErbB4* mutations in PV cells engender a variety of dysfunctions in PV cells including reduced PV presynaptic boutons, mIPSCs, and GAD67 expression. Behaviorally, mice with *ErbB4* mutations display increased locomotor activity and deficits in social and cognitive function, consistent with other mouse models of schizophrenia (del Pino et al., 2013). Most notably, perhaps, they display reduced auditory pre-pulse inhibition, which is considered a hallmark of mouse models of schizophrenia (del Pino et al., 2013).

Lastly, the schizophrenic state is also associated with attenuated gamma oscillations in the frontal and sensory cortices in both humans and mouse models of schizophrenia. This finding is independent of medication usage, which suggests that it may contribute to the disease etiology, further strengthening the tie between PV microcircuit dysfunction and schizophrenia (Lewis et al., 2012). Taken together, work linking PV inhibition to psychiatric disorders, such as autism spectrum disorders and schizophrenia, highlight the fact that normal PV inhibition is essential for normal cortical computation. Furthermore, they underscore the importance of understanding the

development, organization, and function of PV microcircuits, which would not only provide new insights into the etiology of the aforementioned disorders but also suggest novel targets of treatment.

What regulates the development of PV microcircuits?

While the organization of cortical PV microcircuits is relatively well-characterized and the function of PV inhibition is becoming increasingly clear, little is known about the processes, pathways, and molecules that regulate the initial emergence of mature PV microcircuits. A mature PV microcircuit is one that has the correct number and distribution of input as well as the correct number of accurately targeted outputs, especially to pyramidal neurons, the principal downstream targets of PV inhibition.

What is known, however, is that PV microcircuits are especially malleable in response to sensory experience during the critical period, a time during development when experience modulates cortical circuits in general. For example, studies in the primary visual cortex on how dark-rearing, or sensory deprivation, alters the development of orientation selectivity in PV cells suggest that environmental input is needed for the development of the broad-tuning seen in mature PV cells, which in turn is crucial for normal visual processing in V1 (Kuhlman et al., 2011). The critical period in the visual cortex spans from about P21 to P30 and pre-critical period L2/3 PV cells are more sharply tuned than post-critical period PV cells, but they are still significantly less tuned than pyramidal neurons at any given point in time. PV cells in V1 of adult dark-reared

mice, however, have an orientation selectivity similar to that of pre-critical period PV cells, suggesting that the normal broadening of tuning with age is visual experience dependent. However, it is unclear on which segment of the PV microcircuit experience acts and how. Prediction of the former would be difficult, as it would require knowledge of the extent to which feed-forward input versus local circuitry contribute to PV tuning, which is as of yet incomplete. Incidentally, PV cells also increase their firing in response to visual stimuli during the critical period, which then persists into adulthood. This increase in activity can be blocked with sensory deprivation.

Lastly, PV cells also increase their inhibition of surrounding pyramidal neurons at the onset of the critical period, thereby opening the critical period (**Fig. 3**, Hensch et al., 1998; Chattopadhyaya et al., 2004; Fagiolini et al., 2004; Gandhi et al., 2008; Kuhlman et al., 2011; Kuhlman et al., 2013). A survey of PV bouton distribution per pyramidal neuron cell body revealed a significant increase in the density of PV synapses on pyramidal neuron cell bodies between P18 (pre-critical period) and P24 (early critical period), which could be blocked by injecting TTX into the eye and preventing the transduction of light into neural signals, thereby reducing thalamic input to the visual cortex (Chattopadhyaya et al., 2004). Sensory experience, therefore, is required for the development of adequate perisomatic inhibition, which in turn is necessary for critical period plasticity and cortical computation (Hensch et al., 1998; Chattopadhyaya et al., 2004; Fagiolini et al., 2004; Gandhi et al., 2008; Kuhlman et al., 2011; Kuhlman et al., 2013; Isaacson and Scanziani, 2011).

How, then, does sensory experience get transduced into changes in perisomatic inhibition?

This question gets at the molecular pathways and molecules that make wiring changes within PV microcircuits possible. A candidate pathway is the ubiquitous AKT pathway, which regulates gene expression by regulating transcription and translation of transcription factors and whose activity may be cell activity dependent (**Fig. 4**; Zhou and Parada, 2012, Costa-Mattioli and Monteggia, 2013; Garcia-Junco-Clemente and Golshani, 2014). Furthermore, it is strongly implicated in autism spectrum disorders, the social and cognitive deficits of which arise from deficiencies in inhibition. Many notable autism candidate genes, such as *PTEN*, *TSC1,* and *TSC2* converge on the AKT pathway. Loss of function mutations of these genes result in increased AKT pathway activity. In spite of the compelling link between deficits in inhibition and autism and independently, the AKT pathway and autism, nothing is known about how the AKT pathway is related to the genesis or modulation of inhibition.

The pathway has, however, been studied in relation to the structure and function of pyramidal neurons. The AKT pathway has been shown to regulate dendritic development, axonal development, or both of pyramidal neurons depending on the particular form of pathway modulation. A common target of pathway modulation is PTEN (phosphatase and tensin homolog), a phosphatase upstream of the pathway that negatively regulates its activity (**Fig. 4**). If a *Nse-cre* (neuron-specific enolase driven cre) is used to delete both copies of *PTEN* from select heterogeneous neurons in layers III-V of the cortex, parts of the hippocampus (CA3 and PML), and dentate gyrus starting from

the second postnatal week, these neurons display increased dendritic and axonal arborization, as well as somatic hypertrophy (Kwon et al., 2006). In contrast, acute, conditional deletion of both copies of *PTEN* in adult cortical pyramidal neurons via *CamKIIa-cre* results in increased growth of L2/3 apical dendrites only (Chow et al., 2009). Interestingly, a single copy *PTEN* deletion in L2/3 pyramidal neurons via *CamKIIa-Cre* does not alter the structure of pyramidal neurons but decreases their intrinsic excitability by up-regulating the expression SK channels, a calcium dependent potassium channel (Garcia-Junco-Clemente et al., 2013).

Although PTEN and the AKT pathway have never been studied before in any kind of inhibitory neuron, the work on their role in pyramidal neurons suggests that they may regulate some aspect of PV microcircuit assembly. Hence, the incentive for the ensuing work is two-fold: one, whether PTEN and the AKT pathway regulate some aspect of PV microcircuit assembly and two, whether this pathway could be the transducer of sensory experience into the kind of tunable perisomatic inhibition needed for the development of mature PV microcircuits, which in turn would dictate the parameters of cortical computation.

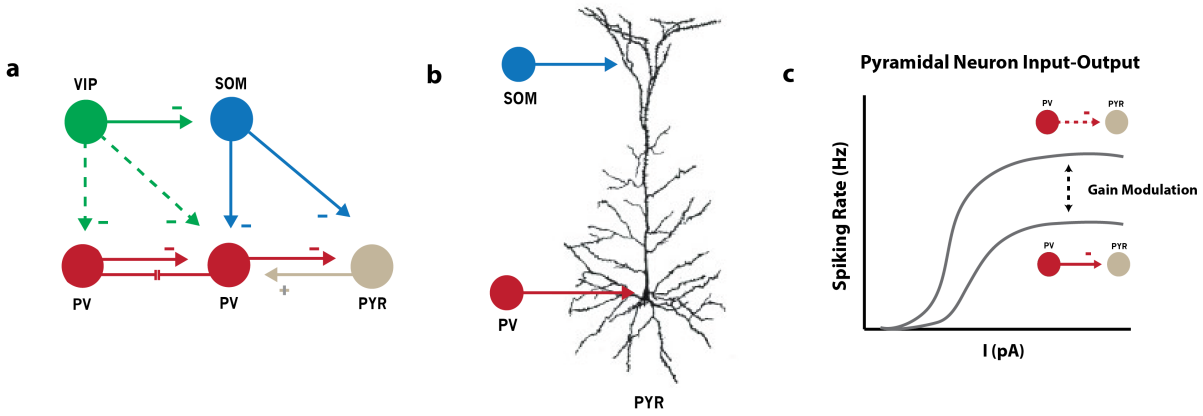

Figure 1| Cortical PV microcircuit and function. a, An intralaminar PV -centric circuit diagram. PV cells receive inhibitory input from other PV cells, SOM neurons and to a marginal extent, VIP neurons. They also receive dense excitatory input from pyramidal neurons. In turn, they inhibit pyramidal neurons and other PV cells. **b,** PV cells supply inhibition to the cell body and axon initial segment of pyramidal neurons, thereby regulating output. In contast, SOM cells inhibit the apical dendrites. **c,** PV cells modulate the gain of pyramidal neurons. A decrease in PV inhibition (dotted line) increases the slope of the input-output curve of pyramidal neurons and hence, increases their excitability.

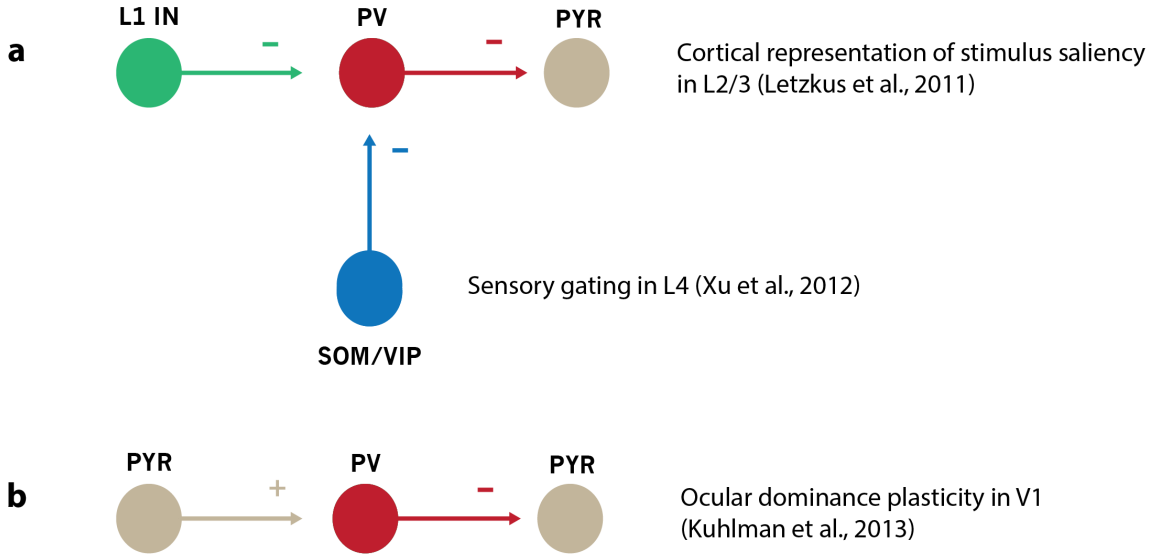

Figure 2| PV cells in disinhibitory circuits. a, Inhibition of inhibition: A L1 inhibitory neuron can disinbhit a L2/3 pyramidal neuron via an intermediary L2/3 PV cell. This is important in coding stimulus saliency in fear conditioning (Letzkus et al., 2011). L4 somatostatin disinhibition of a L4 pyramidal neuron via a L4 PV cell is important in sensory gating (Xu et al., 2012). **b,** Disinhibition can also be mediated by decreased excitatory drive onto PV cells, which would disinhibit downstream pyramidal neurons. This underlies ocular dominance plasticity (Kuhlman et al., 2013).

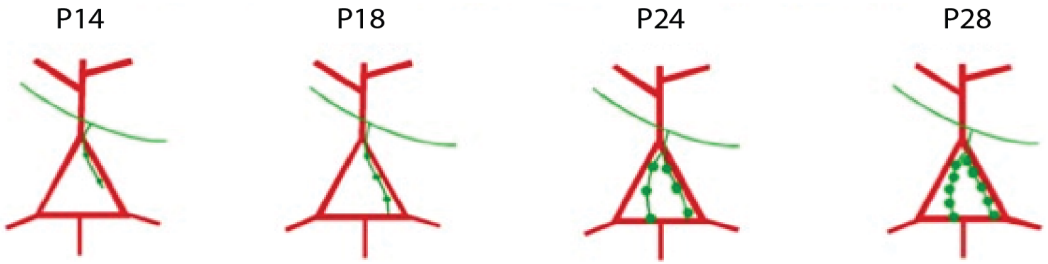

Figure 3| Development of PV inhibition of pyramidal neurons. PV perisomatic inhibition increases significantly at the onset of the critical period (P24). Schematic taken and adapted from Chattopadhyaya et al., 2004.

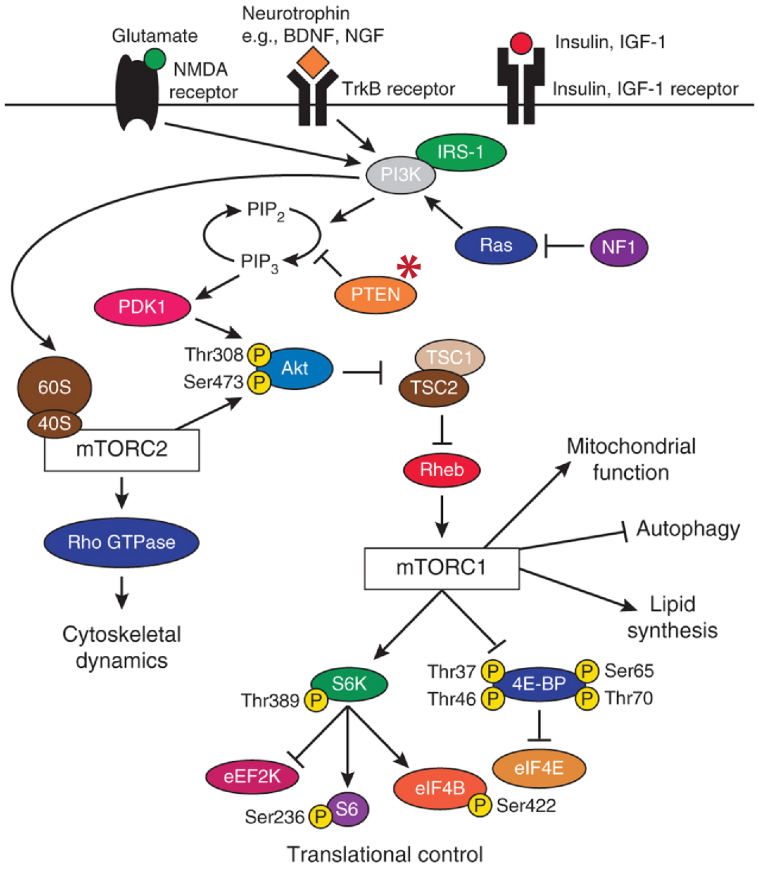

Figure 4| The AKT signaling pathway. This ubiquitous pathay regulates transcription (not shown) and translation. PTEN (red asterix) is a phosphatase that negatively regulates the pathway. A decrease in PTEN expression would increase AKT pathway activity and therefore, transcruption and translation. Schematic taken from Costa-Mattioli and Monteggia, 2013.

References

Abbott, L. F. & Chance, F. S. in *Progress in Brain Research* **149,** 147–155 (2005).

Acsády, L., Görcs, T.J. & Freund, T.F. Different populations of vasoactiveintestinal polypeptide-immunoreactive interneurons are specialized to control pyramidal cells or interneurons in the hippocampus. Neuroscience **73,** 317–334 (1996).

Adesnik, H. & Scanziani, M. Lateral competition for cortical space by layer-specific horizontal circuits. *Nature* **464,** 1155–1160 (2010).

Adesnik, H., Bruns, W., Taniguchi, H., Huang, Z. J. & Scanziani, M. A neural circuit for spatial summation in visual cortex. *Nature* **490,** 226–231 (2012).

Ascoli, G.A. et al. Petilla terminology: nomenclature of features of GABAergic interneurons of the cerebral cortex. Nat. Rev. Neurosci. **9,** 557–568 (2008).

Atallah, B. V. & Scanziani, M. Instantaneous Modulation of Gamma Oscillation Frequency by Balancing Excitation with Inhibition. *Neuron* **62,** 566–577 (2009).

Atallah, B. V. *et al.* Parvalbumin-Expressing Interneurons Linearly Transform Cortical Responses to Visual Stimuli. *Neuron* **73,** 159–170 (2012).

Ayaz, A. & Chance, F. S. Gain Modulation of Neuronal Responses by Subtractive and Divisive Mechanisms of Inhibition. *Journal of Neurophysiology* **101,** 958–968 (2008).

Belmonte, M. K., Gomot, M. & Baron-Cohen, S. Visual attention in autism families: 'unaffected' sibs share atypical frontal activation. *Journal of Child Psychology and Psychiatry* **51,** 259–276 (2010).

Branco, T. & Häusser, M. Synaptic integration gradients in single cortical pyramidal cell dendrites. Neuron **69,** 885–892 (2011).

Bragin, A. *et al.* Gamma (40–100 Hz) oscillation in the hippocampus of the behaving rat. *J. Neurosci* **15**, 47–60 (1995).

Burkhalter, A. Many specialists for suppressing cortical excitation. Front. Neurosci. **2,** 155–167 (2008).

Buzsaki, G., Leung, L.W., Vanderwolf, C.H. Cellular bases of hippocampal EEG in the behaving rat. *Brain Research* **287,** 139–71 (1983).

Buzsáki, G. & Wang, X.-J. Mechanisms of Gamma Oscillations. *Annu. Rev. Neurosci.* **35,** 203–225 (2012).

Canitano, R. Epilepsy in autism spectrum disorders. *Eur Child Adolesc Psychiatry* **16,** 61–66 (2006).

Carandini, M. & Heeger, D. J. Normalization as a canonical neural computation. *Nature Reviews Neuroscience* **13**, 51-63 (2011).

Cardin, J. A. *et al.* Driving fast-spiking cells induces gamma rhythm and controls sensory responses. *Nature* **459,** 663–667 (2009).

Chapman, B. & Stryker, M.P. Origin of orientation tuning in the visual cortex. *Curr Opin Neurobiol,* **2(4):** 498-501 (1992).

Chattopadhyaya, B. Experience and Activity-Dependent Maturation of Perisomatic GABAergic Innervation in Primary Visual Cortex during a Postnatal Critical Period. *Journal of Neuroscience* **24,** 9598–9611 (2004).

Constantinidis, C., Williams, G. V. & Goldman-Rakic, P. S. A role for inhibition in shaping the temporal flow of information in prefrontal cortex. *Nature Neurosci* **5**, 175–180 (2002).

Chen, T.-W. *et al.* Ultrasensitive fluorescent proteins for imaging neuronal activity. *Nature* **499,** 295–300 (2013).

Chow, D. K. *et al.* Laminar and compartmental regulation of dendritic growth in mature cortex. *Nature Neuroscience* **12,** 116–118 (2009).

Costa-Mattioli, M. & Monteggia, L. M. mTOR complexes in neurodevelopmental and neuropsychiatric disorders. *Nature Neuroscience* **16,** 1537–1543 (2013).

Cristo, G. D. *et al.* Subcellular domain-restricted GABAergic innervation in primary visual cortex in the absence of sensory and thalamic inputs. *Nature Neuroscience* **7,** 1184–1186 (2004).

Dávid, C., Schleicher, A., Zuschratter, W. & Staiger, J.F. The innervation of parvalbumin-containing interneurons by VIP-immunopositive interneurons in the primary somatosensory cortex of the adult rat. Eur. J. Neurosci. **25,** 2329–2340 (2007).

DeFelipe, J. *et al.* New insights into the classification and nomenclature of cortical GABAergic interneurons. *Nature Reviews Neuroscience* **14,** 1–15 (2013).

del Pino, I. *et al.* Erbb4 Deletion from Fast-Spiking Interneurons Causes Schizophrenia-like Phenotypes. *Neuron* **79,** 1152–1168 (2013).

Engel, A., Fries, P., Singer, W. Dynamic predictions: oscillations and synchrony in top-down processing. *Nature Reviews Neuroscience* **2**, 704–16 (2001).

Fagiolini, M. *et al*. Specific GABAA circuits for visual cortical plasticity. *Science* **303,** 1681–1683 (2004).

Fanselow, E.E., Richardson, K.A. & Connors, B.W. Selective, state-dependent activation of somatostatin-expressing inhibitory interneurons in mouse neocortex. J. Neurophysiol. **100,** 2640–2652 (2008).

Fino, E. & Yuste, R. Dense Inhibitory Connectivity in Neocortex. *Neuron* **69,** 1188–1203 (2011).

Freund, T.F. & Buzsáki, G. Interneurons of the hippocampus. *Hippocampus* **6,** 347–470 (1996).

Freund, T.F., Katona, I. Perisomatic inhibition. *Neuron* **56,** 33–42 (2007).

Gabernet, L., *et al.*. Somatosensory Integration Controlled by Dynamic Thalamocortical Feed-Forward Inhibition. *Neuron* **48,** 315–327 (2005).

Gandhi, S.P., Yanagawa, Y., Stryker, M.P. Delayed plasticity of inhibitory neurons in developing visual cortex. *PNAS* **105(43),** 16797-802 (2008).

Garcia-Junco-Clemente, P., *et al.* Overexpression of calcium-activated potassium channels underlies cortical dysfunction in a model of *PTEN*-associated autism. *PNAS* **110 (45)**: 18297-18302 (2013).

Garcia-Junco-Clemente, P., Golshani, P. PTEN: A master regulator of neuronal structure, function, and plasticity. *Commun Integr Biol* **7(1),** e28358 (2014).

Gdalyahu, A. *et al.* Associative Fear Learning Enhances Sparse Network Coding in Primary Sensory Cortex. *Neuron* **75,** 121–132 (2012).

Gentet, L. J. *et al*. Membrane Potential Dynamics of GABAergic Neurons in the Barrel Cortex of Behaving Mice. *Neuron* **65,** 422–435 (2010).

Gentet, L. J. *et al.* Unique functional properties of somatostatin-expressing GABAergic neurons in mouse barrel cortex. *Nature Neurosciene* **15,** 607–612 (2012).

Gomot, M., Belmonte, M. K., Bullmore, E. T., Bernard, F. A. & Baron-Cohen, S. Brain hyper-reactivity to auditory novel targets in children with high-functioning autism. *Brain* **131,** 2479–2488 (2008).

Gonchar, Y. & Burkhalter, A. Three Distinct Families of GABAergic Neurons in Rat Visual Cortex. *Cerebral Cortex* **7,** 347-358 (1997).

Hasenstaub, A. *et al.* Inhibitory postsynaptic potentials carry synchronized frequency information in active cortical networks. *Neuron* **47**, 423–35 (2005).

Hensch, T.K., *et al*. Local GABA circuit control of experience-dependent plasticity in developing visual cortex. *Science* **282(5393),** 1504-8 (1998).

Hestrin, S. & Galarreta, M. Electrical synapses define networks of neocortical GABAergic neurons. *Trends in Neurosciences* **28,** 304–309 (2005).

Hofer, S. B. *et al.* Differential connectivity and response dynamics of excitatory and inhibitory neurons in visual cortex. *Nature Neuroscience* **14,** 1045–1052 (2011).

Hubel, D.H, Wiesel, T.N. Receptive Fields of Single Neurones the Cat's Striate Cortex. *J. Physiol* **128**, 574-591 (1959).

Kato, H. K., Gillet, S. N., Peters, A. J., Isaacson, J. S. & Komiyama, T. Parvalbumin-Expressing Interneurons Linearly Control Olfactory Bulb Output. *Neuron* **80,** 1218–1231 (2013).

Kawaguchi, Y. & Kubota, Y. GABAergic Cell Subtypes and their Synaptic Connections in Rat Frontal Cortex. *Cerebral Cortex* **7,** 476-486 (1997).

Kerlin, A. M., Andermann, M. L., Berezovskii, V. K. & Reid, R. C. Broadly Tuned Response Properties of Diverse Inhibitory Neuron Subtypes in Mouse Visual Cortex. *Neuron* **67,** 858–871 (2010).

Kuhlman, S. J., Tring, E. & Trachtenberg, J. T. Fast-spiking interneurons have an initial orientation bias that is lost with vision. *Nature Neuroscience* **14,** 1121–1123 (2011).

Kuhlman, S. J. *et al.* A disinhibitory microcircuit initiates critical-period plasticity in the visual cortex. *Nature* 1–7 (2013).

Kvitsiani, D. *et al.* Distinct behavioral and network correlates of two interneuron types in prefrontal cortex. *Nature* **498,** 363-370 (2013).

Kwon, C.-H. *et al.* Pten Regulates Neuronal Arborization and Social Interaction in Mice. *Neuron* **50,** 377–388 (2006).

Larkum, M.E., Zhu, J.J. & Sakmann, B. A new cellular mechanism for coupling inputs arriving at different cortical layers. Nature **398,** 338–341 (1999).

Larkum, M.E., Nevian, T., Sandler, M., Polsky, A. & Schiller, J. Synaptic integration in tuft dendrites of layer 5 pyramidal neurons: a new unifying principle. Science **325,** 756–760 (2009).

Lee, S., *et al*. The Largest Group of Superficial Neocortical GABAergic Interneurons Expresses Ionotropic Serotonin Receptors. *Journal of Neuroscience* **30,** 16796–16808 (2010).

Lee, S.-H. *et al.* Activation of specific interneurons improves V1 feature selectivity and visual perception. *Nature* **488,** 379–383 (2012).

Lee, S.-H., Kwan, A. C. & Dan, Y. Interneuron subtypes and orientation tuning. *Nature* **508,** E1–E2 (2014).

Letzkus, J. J. *et al.* A disinhibitory microcircuit for associative fear learning in the auditory cortex. *Nature* **480,** 331–335 (2011).

Lewis, D. A., Curley, A. A., Glausier, J. R. & Volk, D. W. Cortical parvalbumin interneurons and cognitive dysfunction in schizophrenia. *Trends in Neurosciences* **35,** 57–67 (2012).

Lien, A. D. & Scanziani, M. Tuned thalamic excitation is amplified by visual cortical circuits. *Nature Neuroscience* **16,** 1315–1323 (2013).

Losonczy, A., Makara, J.K. & Magee, J.C. Compartmentalized dendritic plasticity and input feature storage in neurons. *Nature* **452,** 436–441 (2008).

Ma, W.P.et al. Visual representations by cortical somatostatin inhibitory neurons–selective but with weak and delayed responses. *J Neurosci* **30**, 14371–14379 (2010).

Markram, H. *et al.* Interneurons of the neocortical inhibitory system. *Nature Reviews Neuroscience* **5,** 793–807 (2004).

Niell, C.M., & Stryker, M.P. Highly selective receptive fields in mouse visual cortex. *J Neurosci* **28(30),** 7520-36 (2008).

Okun, M. & Lampl, I. Instantaneous correlation of excitation and inhibition during ongoing and sensory-evoked activities. *Nature Neuroscience* **11,** 535–537 (2008).

Packer, A. M. & Yuste, R. Dense, Unspecific Connectivity of Neocortical Parvalbumin-Positive Interneurons: A Canonical Microcircuit for Inhibition? *Journal of Neuroscience* **31,** 13260–13271 (2011).

Pangratz-Fuehrer, S. & Hestrin, S. Synaptogenesis of Electrical and GABAergic Synapses of Fast-Spiking Inhibitory Neurons in the Neocortex. *Journal of Neuroscience* **31,** 10767–10775 (2011).

Petersen, C.C.H. The functional organization of the barrel cortex. *Neuron* **56,** 339–355 (2007).

Petersen, C. C. H. & Crochet, S. Synaptic Computation and Sensory Processing in Neocortical Layer 2/3. *Neuron* **78,** 28–48 (2013).

Pfeffer, C. K. *et al*. Inhibition of inhibition in visual cortex: the logic of connections between molecularly distinct interneurons. *Nature* **16,** 1068–1076 (2013).

Pi, H.-J. *et al.* Cortical interneurons that specialize in disinhibitory control. *Nature* **503,** 521–524 (2013).

Pouille, F., *et al*. Input normalization by global feedforward inhibition expands cortical dynamic range. *Nature Neuroscience* **12,** 1577–1585 (2009).

Isaacson, J. S. & Scanziani, M. How Inhibition Shapes Cortical Activity. *Neuron* **72,** 231–243 (2011).

Selby, L., Zhang, C. & Sun, Q.-Q. Major defects in neocortical GABAergic inhibitory circuits in mice lacking the fragile X mental retardation protein. *Neuroscience Letters* **412,** 227–232 (2007).

Silberberg, G. & Markram, H. Disynaptic Inhibition between Neocortical Pyramidal Cells Mediated by Martinotti Cells. *Neuron* **53,** 735–746 (2007).

Sippy, T. & Yuste, R. Decorrelating Action of Inhibition in Neocortical Networks. *Journal of Neuroscience* **33,** 9813–9830 (2013).

Sirota, A., *et al*. Entrainment of neocortical neurons and gamma oscillations by the hippocampal theta rhythm. *Neuron* **60**,683–97 (2008).

Sohal, V. S., Zhang, F., Yizhar, O.&Deisseroth, K. Parvalbumin neurons and gamma rhythms enhance cortical circuit performance. *Nature* **459**, 698–702 (2009).

Somogyi, P. A specific 'axo-axonal' interneuron in the visual cortex of the rat. *Brain Res* **136,** 345–350 (1977).

Staiger, J.F., Masanneck, C., Schleicher, A. & Zuschratter, W. Calbindin-containing interneurons are a target for VIP-immunoreactive synapses in rat primary somatosensory cortex. *J Comp Neurol* **468,** 179–189 (2004).

Taniguchi, H., Lu, J. & Huang, Z. J. The Spatial and Temporal Origin of Chandelier Cells in Mouse Neocortex. *Science* **339,** 70–74 (2013).

Wang, Y. *et al.* Anatomical, physiological and molecular properties of Martinotti cells in the somatosensory cortex of the juvenile rat. *The Journal of Physiology* **561,** 65–90 (2004).

Wilson, N. R. *et al*. Division and subtraction by distinct cortical inhibitory networks in vivo. *Nature* **488,** 343–348 (2012).

Xu, X. & Callaway, E.M. Laminar specificity of functional input to distinct types of inhibitory cortical neurons. *J Neurosci* **29,** 70–85 (2009).

Xu, H., Jeong, H.-Y., Tremblay, R. & Rudy, B. Neocortical Somatostatin-Expressing GABAergic Interneurons Disinhibit the Thalamorecipient Layer 4. *Neuron* **77,** 155–167 (2013).

Xu, N.-L. *et al.* Nonlinear dendritic integration of sensory and motor input during an active sensing task. *Nature* **492,** 247–251 (2012).

Yizhar, O. *et al.* Neocortical excitation/inhibition balance in information processing and social dysfunction. *Nature* **477,** 171–178 (2011).

Zhou, J. & Parada, L. F. PTEN signaling in autism spectrum disorders. *Current Opinion in Neurobiology* 1–7 (2012).

Chapter II

PTEN and the emergence of perisomatic inhibition

Cortical parvalbumin (PV)-expressing inhibitory neurons supply diffuse inhibition to pyramidal neuron cell somas and axon initial segments, thereby exerting control over their output. This perisomatic inhibition is necessary for the generation of gamma oscillations, modulation of neural gain, and expression of several forms of plasticity, such as ocular dominance plasticity during development[1-5]. The importance of PV inhibition is highlighted by the fact that a disruption in the balance of somatic inhibition to excitation in a circuit is associated with the social and cognitive deficits seen in autism spectrum disorders and schizophrenia, which can be rescued by restoring PV activity[6]. While the centrality of PV inhibition to normal cortical computation and plasticity is apparent, little is known about the processes that regulate the emergence of mature, functional PV microcircuits[7,8].

The ensuing experiments were initially motivated by our interest in cellular growth pathways in neurons. While dysregulation of these pathways often result in tumorigenesis in most cell types capable of mitosis, in post-mitotic neurons, it is associated with neurologic and psychiatric disorders. One such pathway is the ubiquitous AKT signaling pathway, on which many candidate genes for psychiatric diseases converge[9,10]. PTEN (phosphate and tensin homolog) is a phosphatase upstream of AKT that negatively regulates the pathway activity. *PTEN* mutations are in fact one of the most validated genetic causes of autism spectrum disorders[10]. Given the association between *PTEN* and ASD, growing evidence for impaired inhibition in ASD and other psychiatric disorders, and importance of PV inhibition in cortical circuits, we generated mice in

which a single copy of *PTEN* was selectively mutated in PV cells (PV-PTEN$^{+/-}$) after the second postnatal week[11].

Mutant PV cells displayed a singular reduction in connectivity to genotypically normal pyramidal neurons, while all else in the PV microcircuit remained normal. Paired whole-cell recordings in L2/3 of the visual cortex of adult mice (P42-P56) revealed a 32% reduction in PV to pyramidal connectivity (**Fig. 1a, b**, WT=85%, Het=58%, n=31-33, p=0.025, Fisher's exact test), while reciprocal pyramidal to PV connectivity remained normal (**Fig. 1b**, PYR->PV: WT= 68%, Het=62%, n=31-34, p=0.79, Fisher's exact test). Notably, connectivity between mutant PV cells was equivalent to that of controls (**Fig. 1b**, PV->PV: WT=100%, Het=100%, n=10-20, p=1, Fisher's exact test), indicating that a single *PTEN* mutation in PV cells selectively impairs the establishment or maintenance of PV to pyramidal connections.

A closer inspection of extant connections between mutant PV cells and pyramidal neurons revealed no marked changes in bidirectional synaptic strength or quality relative to controls (**Fig. 2a**, PV -> PYR response #1: WT= 132.07±27.17 pA, n=25, Het= 99.02±25.51 pA, n=14, p>0.05, two-way repeated measures ANOVA; **Fig. 2d**, PV -> PYR PPR: WT= 0.79±0.04, n=25, Het= 0.78±0.04, n=14, p>0.05, two-way ANOVA; **Fig. 2b**, PYR -> PV response #1: WT= -35.82±9.42 pA, Het= -44.66±7.51 pA, n=20, p>0.05, two-way repeated measures ANOVA; **Fig. 2d**, PYR -> PV PPR: WT=0.94±0.09, Het=0.77±0.03, n=20, P>0.05, two-way ANOVA). Likewise, the synaptic strength amongst PV-PV connections in Het animals was equivalent to that of controls (**Fig. 2c**, response #1: WT= 49.05±4.79 pA, n=20, Het= 39.81±9.96 pA, n=10, p>0.05, two-way

repeated measures ANOVA; **Fig. 2d**, PPR: WT= 0.69±0.02, n=20, Het= 0.74±0.06, $p>0.05$, n=10, two-way ANOVA). We also did not find any evidence of changes in intrinsic properties of mutant PV cells (**Supplemental Fig. 1s**, $p>0.05$, n=15, Friedman's ANOVA).

The decrement in PV to pyramidal connectivity was confirmed two-fold. First, inspection of genotypically normal pyramidal neurons in PV-PTEN$^{+/-}$ mice revealed increased excitability of these cells relative to pyramidal neurons of controls (**Fig. 3a**, **b**, n=12, $p<0.05$, Friedman's ANOVA, multiple t-tests, Holm-Sidak correction). This increase in excitability could not be attributed to intrinsic changes, as blocking all synaptic input with antagonists to AMPAR, NMDAR and $GABA_aR$ normalized the excitability (n=12, $p>0.05$, Friedman's ANOVA), which supports the fact that the increase in excitability was due to a decrease in PV mediated inhibition (**Fig. 3b**). Second, we found a reduction in local PV inhibition of pyramidal neurons in PV-PTEN$^{+/-}$ mice with channelrhodopsin circuit mapping (**Fig. 1c**, **Supplemental Fig. 2s**)[12]. We selectively expressed channelrhodopsin-2 in PV cells in PTEN mutant and control mice and then mapped local cortical PV inhibition to individual pyramidal neurons. Specifically, we noted a 50% reduction in total PV input to pyramidal neurons (**Fig. 1c,** n=12, $p<0.01$, Mann-Whitney U test). Taken together, our findings indicate that single copy *PTEN* mutations in PV cells result in the reduction of the number of PV to pyramidal synapses (**Fig. 3a**).

PTEN is known to negatively regulate the AKT signaling pathway, which in turn regulates transcription and translation of transcription factors, which suggests that *PTEN*

deletion could possibly alter the expression of key presynaptic proteins, resulting in reduced formation of PV to pyramidal inhibitory synapses[9]. To screen for such presynaptic proteins in an unbiased manner, we collected RNA from living cortical PV cells harvested from intact adult brains via fluorescence-assisted cell sorting (**Fig. 4a, b**)[13]. Transcript copy number was then quantified with Illumina mouse gene chip arrays. A comparison of PV cells with and without single copy *PTEN* mutations revealed about 20 transcripts whose change in expression met the established criteria for further examination, namely a p-value <0.001. Of these, the majority coded for proteins pertaining to metabolism and were not specific to neurons. However, also among the top 20 was *EphB4* (logFC=0.56, p=0.00039), the change in expression of which we verified with quantitative-RT PCR (**Fig. 4c**, ddCt=1.84). EphB4 is the presynaptic receptor for EphrinB2 and the EphrinB/EphB bidirectional signaling pathway is known to mediate cell-to-cell repulsion during development, regulating such processes as selective crossing of retinal axons at the optic chiasm[14,15]. Increased expression of *EphB4* in PV-PTEN$^{+/-}$ mice could account for the reduction in PV to pyramidal inhibitory synapses via increased repulsion between the presynaptic terminals of PV cells and cell bodies of pyramidal neurons. Immunofluorescent labeling of EphB4 revealed a punctate, perisomatic distribution around pyramidal neurons, consistent with the perisomatic distribution of PV terminals (**Fig. 4d**). Notably, EphB4 expression in normal mice decreases from P16 to P21, which coincides with the onset of the vision dependent critical period (**Fig. 4e**, n=6, p<0.01, Mann-Whitney U test)[16]. Since visual experience increases PV inhibition of pyramidal neurons, our results suggest that this could possibly

be due to the up-regulation of PTEN and down-regulation of EphB4, which would reduce the native synaptic repulsion between PV presynaptic terminals and pyramidal cell somas[16].

In conclusion, a decrease in PTEN expression in PV cells results in an increase in expression of EphB4 in PV presynaptic terminals, which prevents the formation of PV to pyramidal inhibitory synapses via cell-to-cell repulsion. This results in a decrease in PV to pyramidal connectivity in a circuit, which consequently increases the excitability of pyramidal neurons. PTEN, therefore, regulates the formation of adequate perisomatic inhibition of pyramidal neurons via EphB4. Since EphB4 expression decreases at around the onset of the critical period, this may modulate the inception of sensory critical periods by enhancing the inhibition of pyramidal neurons and may in turn be modulated by experience[16,17,18]. Given that sufficient perisomatic inhibition is needed for critical period plasticity and normal cortical computation, deficits in PV to pyramidal connectivity may account for impairments in the normal emergence of social and cognitive abilities in autistic patients[17, 18]. Understanding such a process may therefore reveal novel targets of intervention.

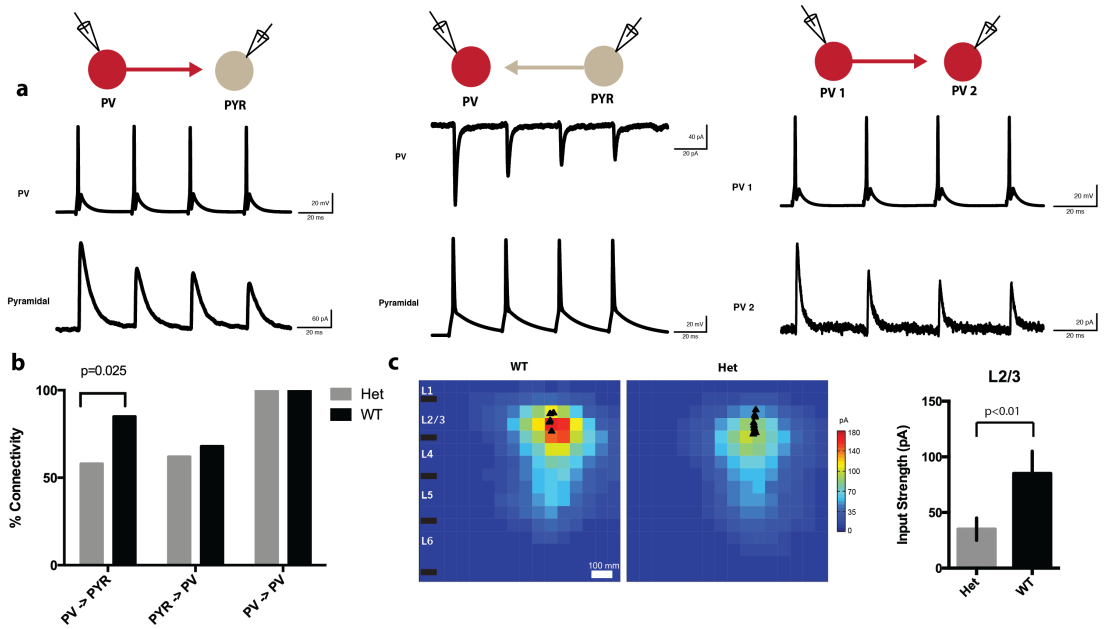

Figure 1| A selective reduction in PV -> PYR connectivity in Hets . **a**, Left, paired recording; an example of a connected PV -> PYR pair. Middle, a connected PYR -> PV pair. Right, a connected PV -> PV pair. **b**, Summary of connectivity for PV-PYR and PV-PV pairs in WT and Het animals. There is a significant reduction in PV -> PYR connectivity in Het mice (p=0.025, n=31-33 pairs, Fisher's exact test). **c**, ChR2 circuit mapping of PV inhibition to L2/3 Pyr neurons in the same region shows a 50% reduction in PV inhibition (p<0.05, n=12 cells, Mann-Whitney U test, mean+/- SEM).

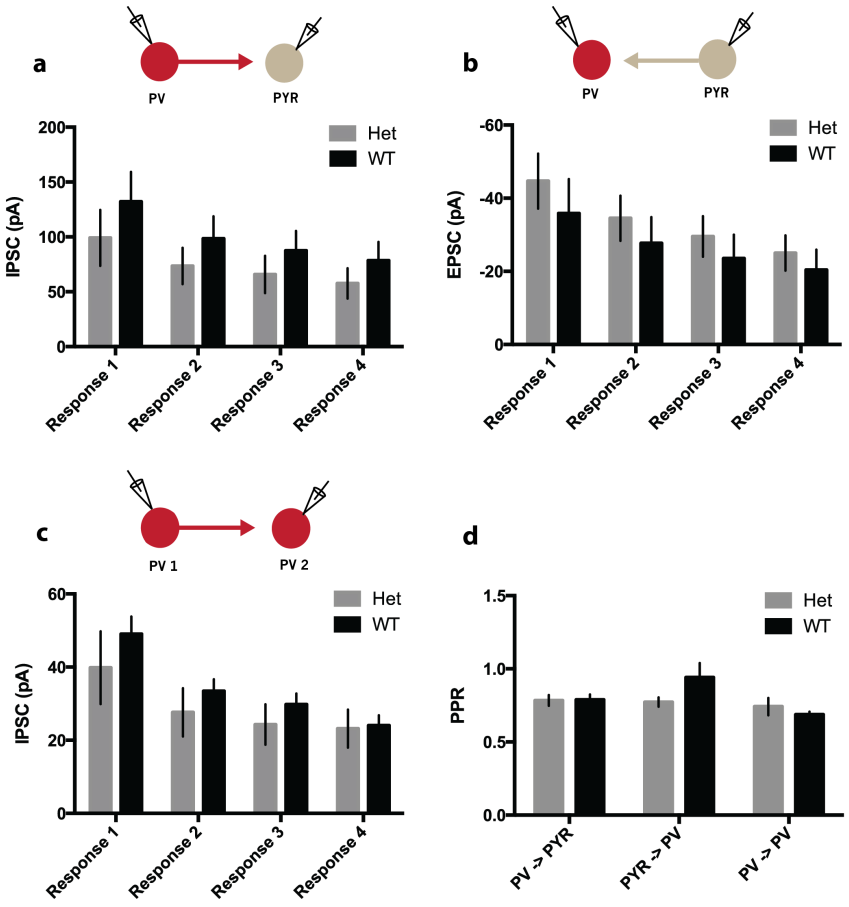

Figure 2| Synaptic strength of extant pairs is normal. a, PV -> PYR IPSC amplitudes of Het mice are similar to that of controls ($p>0.05$, n= 14, two-way rm ANOVA). **b**, PYR -> PV EPSC amplitudes in Het mice are similar to that of controls ($p>0.05$,n=20, two-way rm ANOVA). **c**, Likewise, PV -> PV IPSCs in Het mice are equivalent to that of controls ($p>0.05$, n=20, two-way rm ANOVA). **d**, PPR of all pairs in Hets is equivalent to that of controls ($p>0.05$, two-way ANOVA). Results in mean +/- SEM.

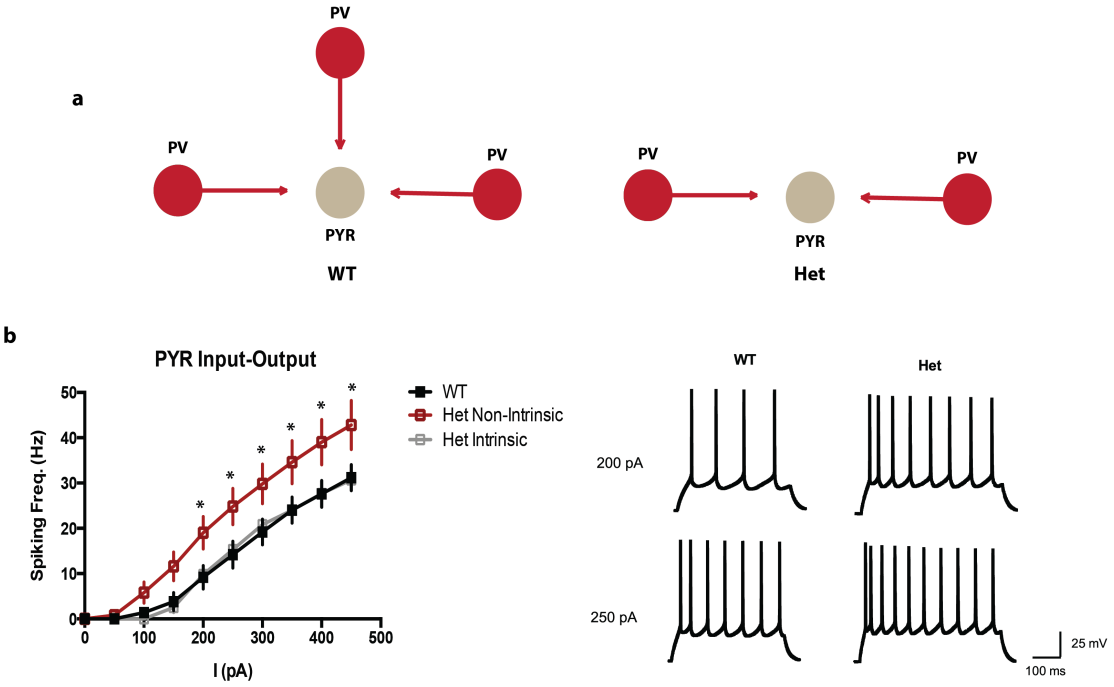

Figure 3| Decreased PV inhibition increases the excitability of PYR neurons. a, A 32% reduction in PV to pyramidal inhibitory connectivity is seen in Het animals. **b,** Left, decreased PV inhibition results in the increased excitability of PYR neurons in Het animals that cannot be attributed to intrinsic changes (* $p<0.05$, n=12, Friedman's ANOVA, multiple t-tests, Holm-Sidak correction, mean +/- SEM). Right , samples traces from WT and Het animals with 200 pA input (top) and 250 pA input (bottom).

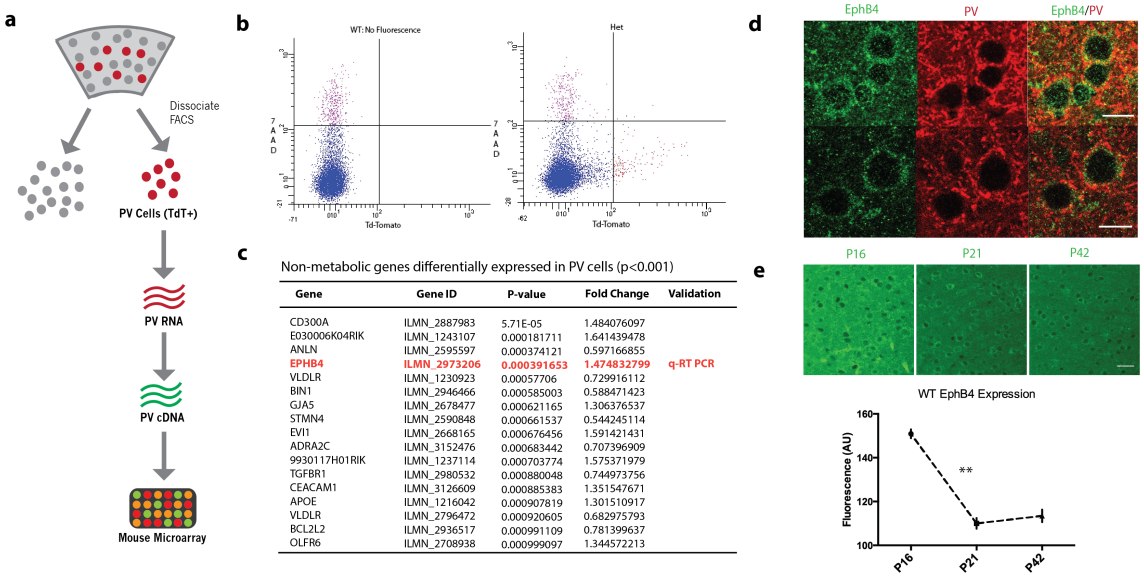

Gene	Gene ID	P-value	Fold Change	Validation
CD300A	ILMN_2887983	5.71E-05	1.484076097	
E030006K04RIK	ILMN_1243107	0.000181711	1.641439478	
ANLN	ILMN_2595597	0.000374121	0.597166855	
EPHB4	**ILMN_2973206**	**0.000391653**	**1.474832799**	**q-RT PCR**
VLDLR	ILMN_1230923	0.00057706	0.729916112	
BIN1	ILMN_2946466	0.000585003	0.588471423	
GJA5	ILMN_2678477	0.000621165	1.306376537	
STMN4	ILMN_2590848	0.000661537	0.544245114	
EVI1	ILMN_2668165	0.000676456	1.591421431	
ADRA2C	ILMN_3152476	0.000683442	0.707396909	
9930117H01RIK	ILMN_1237114	0.000703774	1.575371979	
TGFBR1	ILMN_2980532	0.000880048	0.744973756	
CEACAM1	ILMN_3126609	0.000885383	1.351547671	
APOE	ILMN_1216042	0.000907819	1.301510917	
VLDLR	ILMN_2796472	0.000920605	0.682975793	
BCL2L2	ILMN_2936517	0.000991109	0.781399637	
OLFR6	ILMN_2708938	0.000999097	1.344572213	

Figure 4| EphB4 is regulated by PTEN. a, A schematic of the process used to isolate RNA from adult, living PV cells for gene expression analysis. **b,** FACS signals for a WT mouse with no fluorescent labeling of proteins (left) and a Het animal with Td-Tomato labeling of PV cells. X-axis, 7AAD signal (au); y-axis, Td-Tomato signal (au). **c,** Differential gene expression list of the top non-metabolic genes ($p<0.001$) from mouse microarray experiments. EphB4 is the top, non-metabolic presynaptic protein ($p=0.0004$), the differential expression of which (logF-C=1.47) was verified with q-RT PCR (ddCt=1.84). **d,** EphB4 expression (green) in the WT cortex and co-localization with PV (red), P30, 100X. EphB4 is punctate and perisomatically distributed, just as PV terminals are perisomatically distributed. Scale bar=10um. **e,** EphB4 in WT cortex decreases in expression from P16 to P21 (**$p<0.01$, n=6, Mann-Whitney U test, mean+/- SEM). No discernable changes occur from P21 to P42 ($p>0.05$, n=6, Mann-Whitney U test, mean +/- SEM). Scale bar=30um.

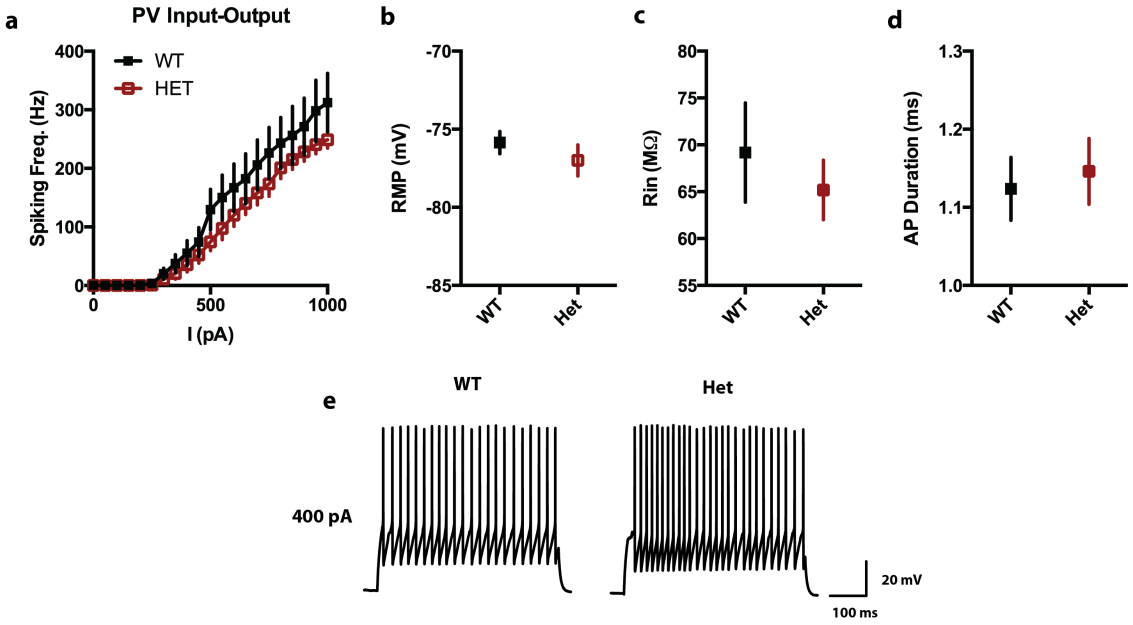

Figure 1s| PTEN mutation in PV cells does not alter intrinsic properties. **a,** Intrinsic excitability of PV cells of Het mice is comparable to that of controls ($p>0.05$, Friedman's ANOVA, n=15). **b**, Resting membrane potential (RMP) of Het PV cells is comparable to that of controls ($p>0.05$, Mann-Whitney U test, n=15). **c**, Input resistance (Rin) of Het PV cells is similar to that of controls ($p>0.05$, Mann-Whitney U test, n=15). **d**, Action potential duration of Het PV cells is also equivalent to that of controls ($p>0.05$, Mann-Whitney U test, n=15). Results in mean +/- SEM.

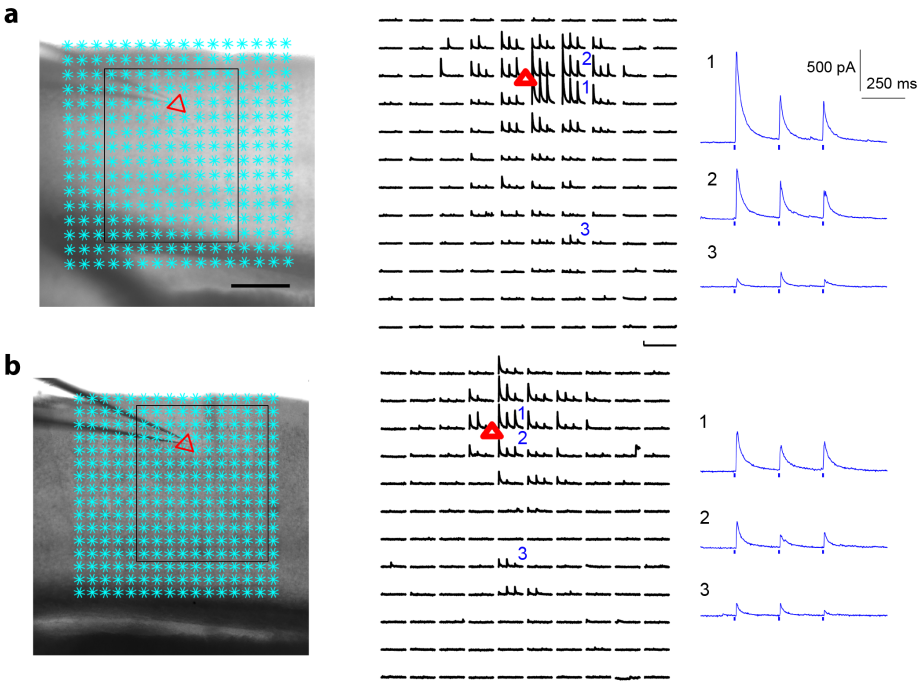

Figure 2s| ChR2 circuit mapping. a, Sample map of a L2/3 cortical pyramidal neuron from a WT mouse (left and middle). Blue grid denotes areas of ChR2 stimulation. Right, sample IPSCs from 3 regions indicated in the middle figure. **b**, Sample map of a cortical L2/3 pyramidal neuron from a Het animal (left and middle). Right, sample IPSCs from 3 regions specified in the middle figure.

References

1. Atallah, B. V. *et al.* Parvalbumin-Expressing Interneurons Linearly Transform Cortical Responses to Visual Stimuli. *Neuron* **73,** 159–170 (2012).

2. Wilson, N. R. *et al*. Division and subtraction by distinct cortical inhibitory networks in vivo. *Nature* **488,** 343–348 (2012).

3. Buzsáki, G. & Wang, X.-J. Mechanisms of Gamma Oscillations. *Annu. Rev. Neurosci.* **35,** 203–225 (2012).

4. Cardin, J. A. *et al.* Driving fast-spiking cells induces gamma rhythm and controls sensory responses. *Nature* **459,** 663–667 (2009).

5. Kuhlman, S. J. *et al.* A disinhibitory microcircuit initiates critical-period plasticity in the visual cortex. *Nature* 1–7 (2013).

6. Yizhar, O. *et al.* Neocortical excitation/inhibition balance in information processing and social dysfunction. *Nature* **477,** 171–178 (2011).

7. Markram, H. *et al.* Interneurons of the neocortical inhibitory system. *Nature Reviews Neuroscience* **5,** 793–807 (2004).

8. Isaacson, J. S. & Scanziani, M. How Inhibition Shapes Cortical Activity. *Neuron* **72,** 231–243 (2011).

9. Costa-Mattioli, M. & Monteggia, L. M. mTOR complexes in neurodevelopmental and neuropsychiatric disorders. *Nature* **16,** 1537–1543 (2013).

10. Zhou, J. & Parada, L. F. PTEN signaling in autism spectrum disorders. *Current Opinion in Neurobiology* 1–7 (2012).

11. Taniguchi, H. *et al.* A Resource of Cre Driver Lines for Genetic Targeting of GABAergic Neurons in Cerebral Cortex. *Neuron* **71,** 995–1013 (2011).

12. Petreanu, L. *et al*. The subcellular organization of neocortical excitatory connections. *Nature* **457,** 1142–1145 (2009).

13. Lobo, M. K. *et al.* FACS-array profiling of striatal projection neuron subtypes in juvenile and adult mouse brains. *Nature Neuroscience* **9,** 443–452 (2006).

14. Nakagawa S. *et al.* Ephrin-B regulates the ipsilateral routing of retinal axons at the optic chiasm. *Neuron* **25**, 599-610 (2000).

15. Williams, S.E. *et al.* Ephrin-B2 and EphB1 mediate retinal axon divergence at the optic chiasm. *Neuron* **39**, 919-935 (2003).

16. Kuhlman, S. J., Tring, E. & Trachtenberg, J. T. Fast-spiking interneurons have an initial orientation bias that is lost with vision. *Nature Neuroscience* **14,** 1121–1123 (2011).

17. Chattopadhyaya, B. Experience and Activity-Dependent Maturation of Perisomatic GABAergic Innervation in Primary Visual Cortex during a Postnatal Critical Period. *Journal of Neuroscience* **24,** 9598–9611 (2004).

18. Hensch, T.K., *et al*. Local GABA circuit control of experience-dependent plasticity in developing visual cortex. *Science* **282(5393),** 1504-8 (1998).

Chapter III

Methods

Mice

Exon 5 of *PTEN* was selectively deleted in PV cells by crossing PV-Cre: Ai9 mice with $PTEN^{flox/flox}$ mice. The deletion occurred around the second postnatal week when *Pvalb* expression began[1]. Only heterozygous animals were used for experiments, as complete exon 5 knock-outs experienced seizures and did not survive past P30. PV-Cre:Ai9 mice were used as controls for all experiments. Cells from C57/BL6 mice without fluorescent proteins were used to calibrate gates in FACS experiments. To selectively express Channelrhodopsin2-YFP in PV cells, we crossed PV-Cre: Ai9: $PTEN^{+/-}$ mice with Ai32 mice. PV-Cre: Ai32 mice from the same litter were used as controls in ChR2 mapping experiments.

Electrophysiology: paired-recordings

Brains were dissected from adult (P35-56) male and female mice. 350 um coronal cortical slices containing the visual cortex were acquired with a Leica vibratome, using a sucrose cutting solution containing 222 mM Sucrose, 11 mM D-Glucose, 26 mM $NaHCO_3$, 1 mM NaH_2PO_4, 3 mM KCl, 7 mM $MgCl_2$ and 0.5 mM $CaCl_2$, continuously oxygenated with 95% O_2 and 5% CO_2. Slices were then incubated at 37°C for 30 minutes in standard ACSF containing 124 mM NaCl, 2.5 mM KCl, 1.25 mM NaH_2PO_4, 10 mM D-Glucose, 4 mM Sucrose, 2.5 mM $CaCl_2$, 2 mM $MgCl_2$, and 26 mM $NaHCO_3$ with continuous oxygenation (95% O_2 and 5% CO_2). All recordings were done in 33-35°C with an internal solution containing 115 mM K-Gluconate, 20 mM KCl, 10 mM HEPES, 10 mM Phosphocreatine, 4 mM ATP-Mg, and 0.3 mM GTP. Pipettes with resistance

between 4-6 MΩ were generated with a P1000 Sutter micropipette puller (Sutter Instruments).

All recordings were done in L2/3 of the visual cortex. Cell bodies were localized with DIC optics on an Olympus BX51 microscope. Only cells >50 um away from the surface of the slice were targeted for whole-cell recordings. Data was acquired and digitized with an Axon 200B amplifier (Molecular Devices) at 15 KHz and then filtered at 8 KHz using MultiClamp (Molecular Devices) and WinWCP. PV cells were identified by their Td-Tomato expression as well as their unique firing pattern, characterized by narrow action potentials, sharp afterhyperpolarizations and fast firing rates[2]. Pyramidal neurons were identified by their lack of Td-Tomato expression, as well as their accommodating and slower firing pattern. Initial assessment of firing pattern was done in current clamp (IC) at resting membrane potential with current injections at 50 pA increments. To generate comparable input-output curves, cells were clamped at -75 mV for 50 pA increment current injections. Intrinsic excitability was assessed in the presence of the following antagonists: 10 uM picrotoxin ($GABA_A$ antagonist), 20 uM CNQX (AMPAR antagonist) and 50 uM APV (NMDAR antagonist). Only cells with Ra <25 MΩ were included in subsequent analysis. R_a was compensated in VC and bridge in IC. Comparison of excitability between WT and Het cells (PV and pyramidal, independently) was performed with Friedman's ANOVA, followed multiple t-tests with Sidak-Holm correction if Friedman's ANOVA yielded $p<0.05$. Intrinsic properties of WT and Het PV cells, such as RMP, Rin, and AP duration was compared with the Mann-Whitney U test, with the threshold for statistical significance set at $p<0.05$.

Assessment of connectivity was done with the presynaptic cell in voltage clamp (VC) and the putative postsynaptic cell in IC. The presynaptic cell was stimulated 4 times at 30 Hz. The postsynaptic cell was clamped at +10 mV for IPSCs and -70 mV for EPSCs. Only pairs separated by <2 cell bodies were recorded. Thirty trials were averaged per unidirectional pair. Data was subsequently processed with Clampfit (Molecular Devices) and then exported to Prism and R for graphing and statistical analysis. Connectivity was calculated as the number of pairs connected divided by the total number of pairs recorded. Fisher's exact test was used to compare WT and Het groups. Amplitude of response was measured as the distance from the baseline to the peak of response. Results were expressed as mean ± SEM. A two-way repeated measures ANOVA was used for each pair type to assess for any difference between the WT and Het groups, with the threshold set at $p<0.05$. Paired pulse ratio (PPR) was calculated by dividing the amplitude of response 1 by that of response 2. Results were expressed as mean ± SEM. A two-way ANOVA was used to assess for any difference between WT and Het groups for all pair types, with the threshold set at $p<0.05$.

Electrophysiology: ChR2 circuit mapping

Slice preparation was similar to that of paired recordings described above. For these experiments, standard ACSF used for recordings also included an AMPAR antagonist (10 uM CNQX), NMDAR antagonist (5 uM CCP) and gap junction antagonist (100 uM carbenoxolone) to block excitatory synaptic transmission and gap junction activity, respectively. ChR2 was activated with 473 nm laser stimulation at 12 Hz

(0.25ms/pulse). ChR2-expressing PV cells were stimulated according to a 16x16 grid, with 65 um^2 spacing to cover V1 from the pia to white matter. Spacing was determined empirically to find the shortest distance between two activation sites such that two adjacent PV cells were stimulated[3]. Pyramidal neurons in L2/3 were identified for whole cell recordings by the lack of YFP and Td-Tomato expression and by their pyramidal shaped cell bodies. In addition, their characteristic firing pattern was verified in IC. They were VC-clamped at +5mV to detect IPSCs. Data was acquired with a Multiclamp 700B amplifier (Molecular Devices) and a custom-modified version of Ephus[4]. Data was digitized at 10 KHz.

ChR2 evoked IPSCs were quantified across the 16x16 grid for each cell and 3 maps were averaged per cell. Averaged maps were then superimposed on DIC images to bin responses according to laminar landmarks. Synaptic events were binned from locations spanning +/- 195 um lateral to the targeted pyramidal neuron location[5]. Data was plotted as the average IPSC amplitude per pixel location, as well as the average (+/- SEM) laminar input from L2/3 PV inhibitory neurons to L2/3 pyramidal neurons. The Mann-Whitney U test was used to assess for any difference between the WT and Het groups, with threshold set at $p<0.05$.

FACS, microarray, q-RT PCR

Brains were dissected from adult mice (P35-P56). 500 um coronal cortical slices containing the visual cortex were acquired with a Leica vibratome with standard ACSF containing 124 mM NaCl, 2.5 mM KCl, 1.25 mM NaH_2PO_4, 10 mM D-Glucose, 4 mM

Sucrose, 2.5 mM $CaCl_2$, 2 mM $MgCl_2$, and 26 mM $NaHCO_3$ with continuous oxygenation (95% O_2 and 5% CO_2). Slices were left to recover in standard ACSF at room temperature for 30 minutes before being transferred to a papain solution (Worthington Biochemicals) and left to incubate in 37°C for 1 hour. Worthington Biochemical Papain kit was used to dissociate individual cells from acute slices, which were then filtered through a 70 um mesh into iced L-15 media containing 1X Pen-Strep, 10 mM HEPES, 25 ug/mL DNase and 1 mg/mL BSA[6]. Cells were treated with 7AAD (1 uL/mL) to label dead cells and were then sorted with an Aria II cell sorter (BD Biosciences) for phycoerythrin (PE) signals (Td-Tomato) and peridinin chlorophyll protein (PerCP) signals (7AAD). Cells from control animals without fluorescent proteins were used to calibrate the gates during each sorting session. Td-Tomato positive, 7AAD negative, living PV cells were collected into L-15 media containing an RNase inhibitor. PV RNA was then purified with a Qiagen RNeasy Mini kit and stored at -80C prior to quantification/qualification with a bioanalyzer. Only samples with RIN>8 were subsequently amplified and reverse-transcribed using the NuGEN Ovation Ultra Low Mass RNA Library prep kit for q-RT PCR and microarray experiments. An Illumina mouse chip was used to quantify transcript copy number. A comparison of mean expression between the WT and Het groups generated a differential gene expression list. A t-test was executed for each probe, with the threshold of significance set at $p<0.001$. LogFC values were calculated as the $\log_2$(Het/WT).

For quantitative- RT PCR, primers for mouse EphB4 and GAPDH (reference) were from obtained from Qiagen. SYBR Green was used to quantify PCR products

(Qiagen). The comparative Ct method was used to quantify the difference in EphB4 expression between WT and Hets. The delta-delta value (ddCt) was calculated as follows:

$$ddCt=2^{[(WT_{EphB4}-WT_{GAPDH})-(Het_{EphB4}-Het_{GAPDH})]}$$

Immunohistochemistry

P16-P42 mice were perfused with 1X PBS followed by 4% PFA. Brains were collected and stored in 4% PFA overnight and then subsequently transferred to a 30% sucrose solution with 0.05% NaN_3 until sectioning. 50 um coronal and sagittal sections were acquired with a cryostat at -21°C. Free-floating sections were washed 3 times with 1X PBS prior to being placed in a 2N HCl solution for 17 mins for antigen retrieval of EphB4. They were subsequently washed 3 times in 1X PBS and blocked with 15% Normal Goat Serum (Cell Signaling Technologies) in 0.5% Triton (Invitrogen)/1X PBS (Ambion) for 1.5 hours at room temperature. The sections were then stored in a solution containing a monoclonal mouse anti-EphB4 primary antibody (1:50, Invitrogen) with 0.5% Triton/1X PBS overnight on a shaker in 4°C. The following day, slices were washed and then incubated with the secondary antibody (Alexa Fluor goat anti-mouse 488; 1:1000, Invitrogen) for 2.5 hours at room temperature on a shaker. Slices were mounted on slides with the Vectashield Mounting Medium (Vector Labs). All developmental time-lapse images were stained at the same time.

Images (20X, 100X) were acquired on a Leica SP5 MP confocal microscope. Developmental time-lapse images were acquired with the same settings. Image analysis was performed in Fiji. Change in WT cortical EphB4 fluorescence throughout

development was assessed with the Mann-Whitney U test, with the threshold for significance set at $p<0.05$.

References

1. Taniguchi, H. *et al.* A Resource of Cre Driver Lines for Genetic Targeting of GABAergic Neurons in Cerebral Cortex. *Neuron* **71,** 995–1013 (2011).

2. Pangratz-Fuehrer, S. & Hestrin, S. Synaptogenesis of Electrical and GABAergic Synapses of Fast-Spiking Inhibitory Neurons in the Neocortex. *Journal of Neuroscience* **31,** 10767–10775 (2011).

3. Hooks, B. M. *et al.* Organization of Cortical and Thalamic Input to Pyramidal Neurons in Mouse Motor Cortex. *Journal of Neuroscience* **33,** 748–760 (2013).

4. Suter, B. A. *et al. Ephus*: multipurpose data acquisition software for neuroscience experiments. *Front. Neural Circuits* **4**, 100 (2010).

5. Shi, Y., Nenadic, Z. & Xu, X. Novel use of matched filtering for synaptic event detection and extraction. *PLoS ONE* **5**, e15517 (2010).

6. Lobo, M. K., Karsten, S. L., Gray, M., Geschwind, D. H. & Yang, X. W. FACS-array profiling of striatal projection neuron subtypes in juvenile and adult mouse brains. *Nature Neuroscience* **9,** 443–452 (2006).

Chapter IV

Conclusion

Summary

Visual experience shortly after eye opening alters the rates and patterns of neuronal firing along all stages of visual processing in the nervous system (Wiesel and Hubel, 1963; Hubel and Wiesel, 1977; Ruthazer and Stryker, 1996; Gordon et al., 1996; Crair, et al., 1998; Gandhi et al., 2005; Trachtenberg et al., 2000; Trachtenberg and Stryker, 2001; Hensch, 2005; Smith and Trachtenberg, 2007; Kuhlman et al., 2011, Espinosa and Stryker, 2012). These visually driven changes drive the establishment of somatic inhibition in the visual cortex (Chattopadhyaya et al., 2004; Kuhlman et al. 2011). My work indicates that visual experience increases the expression of PTEN in cortical PV interneurons, which in turn suppresses protein translation. I also present evidence that the increase in PTEN impairs the expression of EphB4, a known synaptic repulsive factor. This interaction between experience, PTEN, and EphB4 supports a model in which PV cells nerve terminals are initially repulsed from pyramidal cell somas due to the expression of the EphB4. Visual experience negatively regulates the expression of EphB4 in PV cells, thereby removing this repulsive factor from presynaptic terminals. This, in turn, promotes the establishment of robust perisomatic inhibition. This is a simple, and straightforward model in which neural activity is the driver of perisomatic inhibition. This model has the strength of being universally applicable to all cortical regions.

Notably, this model also nicely ties together the previously disparate results that 1) visual experience is necessary for the opening of the critical period for ocular

dominance plasticity in visual cortex, and 2) the establishment of robust perisomatic inhibition is necessary for the opening of the critical period (Gordon and Stryker, 1998; Crair, et al., 1998; Hensch et al., 1998; Chattopadhyaya et al., 2004; Fagiolini et al., 2004; Hensch and Stryker, 2004; Hensch, 2005; Gandhi et al., 2008; Kuhlman et al., 2011; Kuhlman et al., 2013). In my model, visual experience opens the critical period specifically by enhancing the firing rates of PV cells. Importantly, this view is grounded in data recently published from the Trachtenberg lab showing that PV cells are preferentially impacted by vision – vision doubles the firing rates of PV cells, while only modestly improving the firing rates of pyramidal neurons (Kuhlman et al., 2011).

Future directions

Significantly, my model is directly testable. Specifically, we can test this model in mice that have been raised in complete darkness or have had both eyes removed just prior to eye opening. Both conditions are known to prevent the normal establishment of perisomatic inhibition in visual cortex, likely because both conditions prevent the normal increase in PV firing rates that results from vision (Kuhlman et al., 2011). Using channelrhodopsin, we can directly titrate levels of PV firing in the cortex of enucleated mice (in this experiment, enucleation is preferable to dark rearing because dark reared mice still have eyes, and the blue light stimulation of the brain would activate photoreceptors in the eyes of these mice and compromise the interpretation of the data sets). The prediction is that perisomatic innervation would develop fairly robustly in enucleated mice when PV cell activity is artificially enhanced by ChR2 stimulation. This

is readily accomplished by breeding PV-Cre mice with the Ai32 line of mice that express ChR2 in the Rosa26 locus. Offspring will express ChR2 solely in PV cells. Indeed, we have already used such mice in our ChR2 mapping studies. This is a technically demanding study, primarily because it is not likely to be sufficient to simply impose a high spike rate on the PV cells using ChR2. Instead, one would need to induce a spike rate that mimics the firing patterns of PV cells when alert mice are viewing naturalistic stimuli (Cang et al., 2005; Wyatt et al., 2012). Thus, prior to undertaking the ChR2 experiments, one would first have to make a large number of targeted recordings from PV cells in alert mice, then model a "naturalistic" firing pattern, then impose this pattern onto PV cells in enucleated mice. The controls for this experiment are also somewhat challenging. We have thought about this at some length, and the correct control is one where we record the firing patterns of PV cells in dark reared mice (not viewing anything), then impose this pattern onto PV cells in enucleated mice using ChR2 stimulation. This will control for the surgeries, enucleation, and blue light stimulation.

The remaining variable is the total amount of activity driven by ChR2 stimulation, which, we hypothesize, is the determining factor in the establishment of perisomatic innervation. To measure this, we could simply cut living sections from these mice, patch pyramidal neurons in layer 2/3 of visual cortex, and perform the same ChR2-mediated mapping studies used in Chapter 2 to quantify the strength of PV input to pyramidal neurons in PTEN het mice. In other mice, we could use immunostaining for PTEN and EphB4 to determine whether PV activity per se is sufficient to increase PTEN expression and decrease EphB4 expression. We showed in Chapter 2 that immunostaining

convincingly reveals the expression level and location of EphB4. Thus, ChR2-mediated stimulation of PV cells in enucleated mice directly tests 1) whether PV activity per se is sufficient to drive the formation of perisomatic innervation, 2) whether PV activity per se is sufficient to cause a decrease in EphB4 expression in PV cell nerve terminals.

There are, however, a number of remaining unknowns. At what age should the stimulation start? When should it stop? A priori, I think a good first experiment is to begin the ChR2 stimulation at postnatal day 19, when in vivo recordings show that PV firing rates are still immature, and continue until P24, when PV firing rates are known to be mature (Kuhlman et al., 2011). Should this prove fruitful, it would be interesting to continue these experiments with even shorter periods of stimulation to determine the minimum amount of activity necessary. Another interesting possibility is that neural activity simply sets the ball in motion. That is, perhaps neural activity is simply needed turn on PTEN activity, and then is no longer needed thereafter for the continued maturation of perisomatic inhibition. This would be quite interesting. Indeed, there is some precedent for such systems in the visual cortex. Loss of vision to one eye is the basis of ocular dominance plasticity, but if cats are placed in darkness after a brief period of unilateral vision, plasticity continues, even though the visual driving force is absent (Hubel et al., 1977; Wiesel and Hubel, 1963; Gordon and Stryker, 1996; Hensch, 2005). Additionally, mice with a full deletion of GAD65, one of two enzymes that produce GABA, do not have a critical period because it fails to open due to poor perisomatic inhibition (Hensch et al., 1998). A single dose of the use-dependent GABA agonist Diazepam is sufficient to trigger a critical period (Hensch et al., 1998; Kuhlman et al.,

2013). Continued inhibition, thereafter, is not needed. Thus, inhibition appears to be a triggering event rather than a guiding factor.

Beyond the role of activity in driving this process, we need also show, directly, that EphB4 expression is the master regulator of perisomatic inhibition. Our immunostaining results in Chapter 2 show that there is a progressive decrease in EphB4 expression that begins at the onset of the critical period for ocular dominance plasticity. If, in fact, this decrease in EphB4 expression is the catalyst for the proliferation of PV perisomatic inhibition of pyramidal neurons, then it follows that over-expressing EphB4 in normal mice raised with normal vision will prevent the normal formation of perisomatic inhibition. To do this, we have engineered an AAV2 virus containing a vector with flexed mouseEphB4, a self-cleaving 2A peptide, and the gene encoding the red fluorescent protein mCherry, all driven by the Synapsin promoter (AAV2/1-Syn.flex.mCherry-T2A-mEphB4). The T2A peptide promotes bicistronic expression of EphB4 and mCherry in the same cells.

Our goal is to inject this virus in the visual cortex of PV-Cre:Ai32 mice (mice expressing ChR2 in PV cells) at postnatal day 14, prior to the maturation of perisomatic inhibition (Kuhlman et al., 2011). After a 2-week incubation period (P28, when perisomatic inhibition is known to be mature), we will cut sections and again use ChR2-mediated circuit mapping to measure the strength and extent of PV input to pyramidal neurons in control (mice receiving AAV without EphB4) and experimental mice (those

receiving AAV-flex.EphB4). We predict that perisomatic inhibition will be significantly reduced in circuits where PV cells over-express EphB4.

PTEN and EphB4 signaling in tumors.

We are not the first group to propose an interaction between PTEN expression and EphB4 signaling. PTEN mutations are common in prostate cancer. In these tumors, EphB4 protein levels are far higher than in normal tissue or in benign tumors (Xia et al., 2005). PTEN mutations are involved in tumor angiogenesis, and this, again, is thought to be caused by enhanced EphB4 expression (Karar and Maity, 2011). To be sure, the literature linking PTEN to EphB4 is sparse, but it is clear that the link is there. Ours are the first findings to define this link in the cortex, and to define how this link regulates neural circuit development.

Our findings in the context of other research on perisomatic inhibition

A large body of work convincingly demonstrates that the maturation of perisomatic inhibition is needed for the opening of critical periods of cortical plasticity (Hensch et al., 1998; Chattopadhyaya et al., 2004; Fagiolini et al., 2004; Gandhi et al., 2008; Kuhlman et al., 2011; Kuhlman et al., 2013). How this perisomatic inhibition develops has been intensively studied, yet our understanding of this issue remains almost entirely incomplete. Two lines of work identify the transcription factor Otx2 and the neurotrophin BDNF (Brain-Derived Neurotrophic Factor) (Huang et al., 1999; Sugiyama et al., 2008). Otx2 is supposedly produced in the retina and transported trans-synaptically

to the thalamus, and then again trans-synaptically to the cortex where it is sequestered in the perineural glycoprotein network on the surface of PV cells, permitting the specific, constitutive capture of Otx2 by PV cells (Sugiyama et al., 2008). Internalization of Otx2 promotes the maturation of PV cells and, presumably, their synapses onto local pyramidal neurons (Sugiyama et al., 2008). One downfall with this hypothesis is that all cortical areas have critical periods (Stern et al., 2001; Bender et al., 2003). Thus, for this model to work across cortical areas, similar trans-synaptic shuttling of transcription factors to PV cells must occur. This seems unlikely. The more parsimonious model, which we propose, is that the activity of PV cells determines the extent of their synaptic input to local pyramidal neurons via suppression of EphB4.

A second finding is that over-expression of BDNF promotes the maturation of PV cells and their synapses. This finding was made in mice that expressed an additional copy of BDNF in cortical pyramidal neurons (via CamKIIa promoter driven expression of a BDNF transgene) (Huang et al., 1999). Thus, BDNF was not expressed in the PV cells. It is clear that BDNF over-expression in pyramidal neurons accelerates the maturation of PV cell synapses, but beyond that, it is not understood how BDNF does so (Huang et al., 1999). PV cells do express TrkB, the receptor for BDNF. But, oddly, BDNF may act to *decrease* the excitability of PV cells, at least in the dentate gyrus (Nieto-Gonzalez and Jensen, 2013), which does not fit our model.

It is possible that there is some interaction between BDNF signaling and PTEN/AKT pathways in PV cells. But BDNF would have to work in an odd way for this to be true. Normally, when BDNF binds a receptor tyrosine kinase (RTK), it activates

the AKT pathway (Chao, 2003; Park and Poo, 2012). For BDNF to fit into our model, activation of the RTK would need to *suppress* the AKT pathway. This is not entirely far-fetched. Results from our own lab show that PTEN deletion in pyramidal neurons has almost nothing in common with PTEN deletion in PV cells, suggesting that the AKT pathway in these two cell types is activating or suppressing a host of unique proteins (Chow et al., 2009; Garcia-Junco-Clemente et al., 2013).

Lastly, it is equally possible that BDNF does not directly bind PV cells in cortex. Perhaps BDNF binds TrkB receptors on other pyramidal neurons, causing them to either release less EphrinB2, the ligand for EphB4, or, alternatively, to express a synaptic attraction signal to PV cells (Palmer and Klein, 2003). This last possibility, if true, would indicate that two pathways are at work – one a reduction of a repulsive factor (here, EphB4 is reduced by activity in our model), and the other an enhancement of a synaptic attractive signal. This would suggest a "push-pull" model of perisomatic inhibition.

Implications for neurological and psychiatric disorders

Deficits in perisomatic inhibition are under intense scrutiny in epilepsy and psychiatric disorders, such as autism spectrum disorders and schizophrenia. Such deficits can arise from intrinsic problems in PV cells resulting in decreased excitability of PV cells or a reduction in PV presynaptic release of GABA. Alternatively, a reduction in PV to pyramidal connectivity, as our results show, could also result in diminished perisomatic inhibition and disrupt the balance of excitation to inhibition in a circuit. Furthermore, deficits in PV to pyramidal connectivity would undermine critical period

plasticity and impair the normal emergence of social and cognitive skills in childhood, as is observed in children with autism spectrum disorders. Hence, it has not escaped our notice that EphB4 may be a novel target of therapy for disorders that arise from deficits in inhibition. Down-regulating EphB4 expression would increase perisomatic inhibition, re-balance excitation to inhibition in cortical circuits, and permit the normal course of critical period plasticity, which would then allow for normal cortical function.

References

Bender, K.J., Rangel, J., Feldman, D.E. Development of columnar topography in the excitatory layer 4 to layer 2/3 projection in rat barrel cortex. *J Neurosci* **23**:8759–8770 (2003).

Cang, J. *et al.* Development of precise maps in visual cortex requires patterned spontaneous activity in the retina. *Neuron* **48(5)**, 797-809 (2005).

Chao, M.V. Neurotrophins and their receptors: A convergence point for many signaling pathways. *Nature Reviews Neuroscience* **4,** 299-309 (2003).

Chattopadhyaya, B. Experience and Activity-Dependent Maturation of Perisomatic GABAergic Innervation in Primary Visual Cortex during a Postnatal Critical Period. *Journal of Neuroscience* **24,** 9598–9611 (2004).

Crair, M.C., Gillespie, D.C., Stryker, M.P. The role of visual experience in the development of columns in cat visual cortex. *Science* **279(5350),** 566-70 (1998).

Chow, D. K. *et al.* Laminar and compartmental regulation of dendritic growth in mature cortex. *Nature Neuroscience* **12,** 116–118 (2009).

Espinosa, J.S. & Stryker, M.P. Development and plasticity of the primary visual cortex. *Neuron* **52(2)**, 230-249 (2012).

Fagiolini, M. *et al.* Specific GABAA circuits for visual cortical plasticity. *Science* **303**, 1681–1683 (2004).

Gandhi S.P., Cang, J., Stryker, M.P. An eye-opening experience. *Nat Neurosci* **8(1)**, 9-10 (2005).

Gandhi, S.P., Yanagawa, Y., Stryker, M.P. Delayed plasticity of inhibitory neurons in developing visual cortex. *PNAS* **105(43),** 16797-802 (2008).

Garcia-Junco-Clemente, P., *et al.* Overexpression of calcium-activated potassium channels underlies cortical dysfunction in a model of *PTEN*-associated autism. *PNAS* **110 (45)**: 18297-18302 (2013).

Gianfranceschi, L., *et al.* Visual cortex is rescued from the effects of dark rearing by overpexresson of BDNF. *PNAS* **100(21),** 12486-12491 (2003).

Gordon, J.A. & Stryker, M.P. Experience-dependent plasticity of binocular responses in the primary visual cortex of the mouse. *J Neurosci* **16(10)**, 3274-86 (1996).

Hensch, T.K., *et al.* Local GABA circuit control of experience-dependent plasticity in developing visual cortex. *Science* **282(5393),** 1504-8 (1998).

Hensch T.K. & Stryker, M.P. Columnar architecture sculpted by GABA circuits in developing cat visual cortex. *Science* **303(5664),** 1678-81 (2004).

Hensch, T.K. Critical period plasticity in local cortical circuits. *Nat Rev Neurosci* **6**, 877–888 (2005).

Hanover, J.L., *et al.* Brain-derived neurotrophic factor overexpression induces precocious critical period in mouse visual cortex. *J Neurosci* **19(22)**, 1-6 (1999).

Huang, Z.J., *et al.* BDNF regulates the maturation of inhibition and the critical period of plasticity in the mouse visual cortex. *Cell* **(98)**, 739-755(1999).

Hubel, D.H., Wiesel, T.N., LeVay, S. Plasticity of ocular dominance columns in monkey striate cortex. *Phil. Trans. R. Soc. Lond.* **278,** 377-409 (1977).

Karark, J., Maity, A. PI3K/AKT/mTOR pathway in angiogenesis. *Frontiers in Molecular Neuroscience* 1–8 (2011).

Kuhlman, S. J., Tring, E. & Trachtenberg, J. T. Fast-spiking interneurons have an initial orientation bias that is lost with vision. *Nature Neuroscience* **14,** 1121–1123 (2011).

Kuhlman, S. J. *et al.* A disinhibitory microcircuit initiates critical-period plasticity in the visual cortex. *Nature* 1–7 (2013).

Nieto-Gonzalez, J. L. & Jensen, K. BDNF Depresses Excitability of Parvalbumin-Positive Interneurons through an M-Like Current in Rat Dentate Gyrus. *PLoS ONE* **8,** e67318 (2013).

Palmer, A. & Klein, R. Multiple roles of ephrins in morphogenesis, neuronal networking and brain function. *Genes Dev* **17,** 1429-1450.

Park, H. & Poo, M. Neurotrophin regulation of neural circuit development and function. *Nature Reviews Neuroscience* **14,** 7-23 (2012).

Ruthazer, E.S. & Stryker, M.P. The role of activity in the development of long-range horizontal connections in are 17 of the ferret. *J Neurosci* **16(22)**, 7253-69 (1996).

Smith, S.L. & Trachtenberg, J.T. Experience-dependent binocular competition in the visual cortex begins at eye opening. *Nature Neuroscience* **10(3),** 370-375 (2007).

Stern, E.A., Maravall, M., Svoboda, K. Rapid development and plasticity of layer 2/3 maps in rat barrel cortex in vivo. *Neuron* **31**, 305–315 (2001).

Sugiyama, S. *et al.* Experience-Dependent Transfer of Otx2 Homeoprotein into the Visual Cortex Activates Postnatal Plasticity. *Cell* **134,** 508–520 (2008).

Trachtenberg, J.T., Tepel, C., Stryker, M.P. Rapid extragranular plasticity in the absence of thalamocortical plasticity in the developing primary visual cortex. *Science* **287(5460),** 2029-2032 (2000).

Trachtenberg, J.T. & Stryker, M.P. Rapid anatomical plasticity of horizontal connections in the developing visual cortex. *J Neurosci* **21(10)**: 3476-82 (2001).

Wiesel, T.N. & Hubel D. H. Single-cell responses in striate cortex of kittens deprived of vision in one eye. *J Neurophysiol* **26**, 1003-1017 (1963).

Wyatt, R. M., Tring, E. & Trachtenberg, J. T. Pattern and not magnitude of neural activity determines dendritic spine stability in awake mice. *Nature Neuroscience* 1–4 (2012).

Xia, G., *et al.* EphB4 expression and biological significance in prostate cancer. *Cancer Research* **65(1),** 4623-32 (2005).